IEEE Access
Multidisciplinary | Rapid Review | Open Access Journal

Received 15 April 2023, accepted 8 May 2023, date of publication 16 May 2023, date of current version 24 May 2023.

Digital Object Identifier 10.1109/ACCESS.2023.3276928

RESEARCH ARTICLE

Impact of Electric Vehicle Charging on Power Distribution Systems: A Case Study of the Grid in Western Kentucky

PRANOY ROY[1], (Member, IEEE), REZA ILKA[1], (Graduate Student Member, IEEE), JIANGBIAO HE[1], (Senior Member, IEEE), YUAN LIAO[1], (Senior Member, IEEE), AARON M. CRAMER[1], (Senior Member, IEEE), JUSTIN MCCANN[2], (Member, IEEE), SAMUEL DELAY[3], STEVEN COLEY[3], MELISSA GERAGHTY[4], AND SACHINDRA DAHAL[4]

[1]Department of Electrical and Computer Engineering, University of Kentucky, Lexington, KY 40506, USA
[2]West Kentucky Rural Electric Cooperative Corporation, Mayfield, KY 42066, USA
[3]Tennessee Valley Authority (TVA), Knoxville, TN 37902, USA
[4]Electric Power Research Institute (EPRI), Charlotte, NC 28262, USA

Corresponding author: Jiangbiao He (Jiangbiao@ieee.org)

The work presented in this paper is based on the project financially supported by Tennessee Valley Authority (TVA) in 2022.

ABSTRACT With the growing adoption of both residential and commercial electric vehicles (EV) and the rapid deployment of EV charging stations, it is of paramount importance to assess the potential overloading impact of intensive EV charging on the operation and planning of power distribution systems. Targeting at the west Kentucky rural area, this research leverages the Distribution Resource Integration and Value Estimation (DRIVE) and HotSpotter software tools to investigate the potential impact of EV charging on the operation of regional distribution systems and the lifetime degradation of power transformers. The research outcome helps identify possible distribution system overload risks and mitigation solutions to meet future intensive EV charging necessity under assumed EV adoption scenarios. Possible overloading in the distribution systems and undervoltage violations are examined. In addition, the overload impact of EV charging is investigated by conducting a multi-physics reliability analysis of a distribution transformer.

INDEX TERMS Electric vehicles, charging infrastructure, overloading, power distribution system, transformer reliability.

I. INTRODUCTION

Electric vehicles (EV), specifically including battery EVs (BEV) and plug-in hybrid EVs (PHEV), are generally charged through the utility grid. Currently, there are more than 100,000 publicly available charging outlets across the United States, and many more charging units will be installed over the next decade. Table 1 summarizes the characteristics and implementation cost of three various types of EV charging units [1]. However, intensive charging during peak power demand time may cause overload in the regional power distribution system, which has not received sufficient attention in the literature.

Increased EV charging induces a lot of challenges for the power distribution systems (PDS). EV charger load can be responsible for reducing the stability of the PDS. Uncontrolled EV charging might lead to a total blackout if it is carried out during peak load periods. For instance, a 10% increase in EV charging load penetration can result in an 18% increase in the PDS demand [2]. Different levels of EV penetration also exhibit the PDS thermal overloading trend, which may lead to decreased transformer performance. When the penetration of EV chargers increases from 20% to 80%, the grid voltage deviation is affected in the range of 12.7% to 43.3% [2]. EV charger penetration also incurs voltage

The associate editor coordinating the review of this manuscript and approving it for publication was Junho Hong.

TABLE 1. EV charging options [1].

Charger type	Ratings	Typical charging time	Cost for equipment and installation
Level 1	120 V, 1.3-2.4kW	2-5 miles of range per hour of charging	$0 to $1,800
Level 2	208-240V, 2.9-19.2kW	10-30 miles of range per hour of charging	$800 to $33,000
DC Fast charging	400-900V, 25-250kW	100-200 miles of range in 30 minutes	$30,000 to $120,000

deviation, leading to poor power factor (PF) and unbalancing in the PDS. The non-linear power electronics associated with the EV chargers are responsible for increasing the harmonics content in grid current, which can deteriorate the PF and the different assets of the utility. A study performed in [3] shows that the EV chargers increase the RMS value of grid line current, which in turn increases the grid losses by approximately 40% during the off-peak charging period and around 62% during the peak charging period. In the literature, various strategies are proposed and discussed to reduce the aforementioned negative impacts of EV chargers on the PDS, including designing a well-planned, coordinating EV charging scheme, incorporating the smart metering system, and adopting sophisticated modulation techniques and input line filters for ameliorating power conditioning [4].

The impact of EV charging on power distribution systems has been explored in the literature. To examine the effects of EV on PDS, battery capacity, state of charge (SOC), and daily energy consumption of EVs have been predicted based on the behavior of EV owners [5]. The negative impacts of EV charging on PDS were investigated in [6], and an automated controller was proposed to meet the customer demand while taking system voltage and battery state of charge into account. Additionally, a smart load management method to regulate EV charging has been explored in [7] to reduce power losses. One controlled charging strategy has been proposed in [8] to increase EV penetration by taking into account voltage and power constraints. In [9], one regulated EV charging method has been devised to lower overall charging costs while complying with the distribution network limits. The authors in [10] investigated a multi-agent control charging approach to regulate the transformer loading and voltage limits. The authors discussed one optimal charging approach in [11] and one smart charging technique in [12] to regulate the transformer voltage and phase unbalance constraints. One systematic method was studied in [13] to understand the grid impacts of heavy-duty charging stations by considering the placement of the charging station. The authors conducted one case study to investigate the impact of EV charging load on the California distribution network, and it was concluded that EV charging load could have a significant impact on the PDS [14].

Various techniques are documented in past studies to compute the maximum penetration level of EV a PDS can handle. The maximum amount of EV loads that can be supported by the grid side's available resources under a completely controlled charging scenario was calculated by the authors in [15] using reliability-based criteria. In [16], one sensitivity indices-based approach was explored to determine the increasing EV demand in specific PDS locations. The authors studied one method for predicting the PDS capacity for accommodating the increased EV demand while maintaining operational limits [17]. In [18] and [19], the probabilistic strategy was utilized to calculate the maximum penetration level of EV to the PDS while ensuring its feasible operation. The authors in [20] identified a few common issues and errors when performing hosting capacity studies and proposed a few techniques to address these errors and improve the accuracy of hosting capacity outcomes. In [21] the hosting capacity of EVs was investigated in order to predict whether the charging demand from EVs can be accommodated by the PDS while taking power quality issues into account (waveform distortion, power system stability, and RMS voltage).

To further investigate the impact of EV charging on the PDS operation and planning, Distribution Resource Integration and Value Estimation (DRIVE), a software tool developed by Electric Power Research Institute (EPRI) in the USA, is used in this work to evaluate the capacity of representative feeders of a Western Kentucky distribution system, in order to meet future EV charging necessity under assumed EV adoption scenarios [22]. Potential overloading (i.e., thermal congestion) on the distribution system and undervoltage violations are investigated. Additionally, the impact of EV intensive charging on distribution transformers has been examined. An EPRI software tool HotSpotter based on a probabilistic method is employed to assess the system-wide impact of EV charging on residential distribution transformers. A distribution transformer rated at 100 kVA is considered as a case study to characterize the impact of system overload due to EV charging on distribution transformers. Multi-physics analysis is carried out to show the impact of overload on transformer hotspot temperature (HST) and the lifetime degradation.

While there are papers analyzing EV penetration impacts on PDS using small IEEE test systems, this paper intends to propose a systematic method to study EV penetration impacts on real world power grids, considering EV adoption prediction and EV charging profiles, impacts of time-of-use electricity rate, probabilistic analysis of EV charging on distribution transformers, and finite element analysis of overloading impact on distribution transformer aging. As more and more EVs are integrated into power distribution systems, it will be of paramount interest to investigate the potential impact on the distribution grid and its power apparatuses. West Kentucky Rural Electric Cooperative Corporation (WKRECC) has deployed advanced metering infrastructure system so that it has load data available for analysis. That

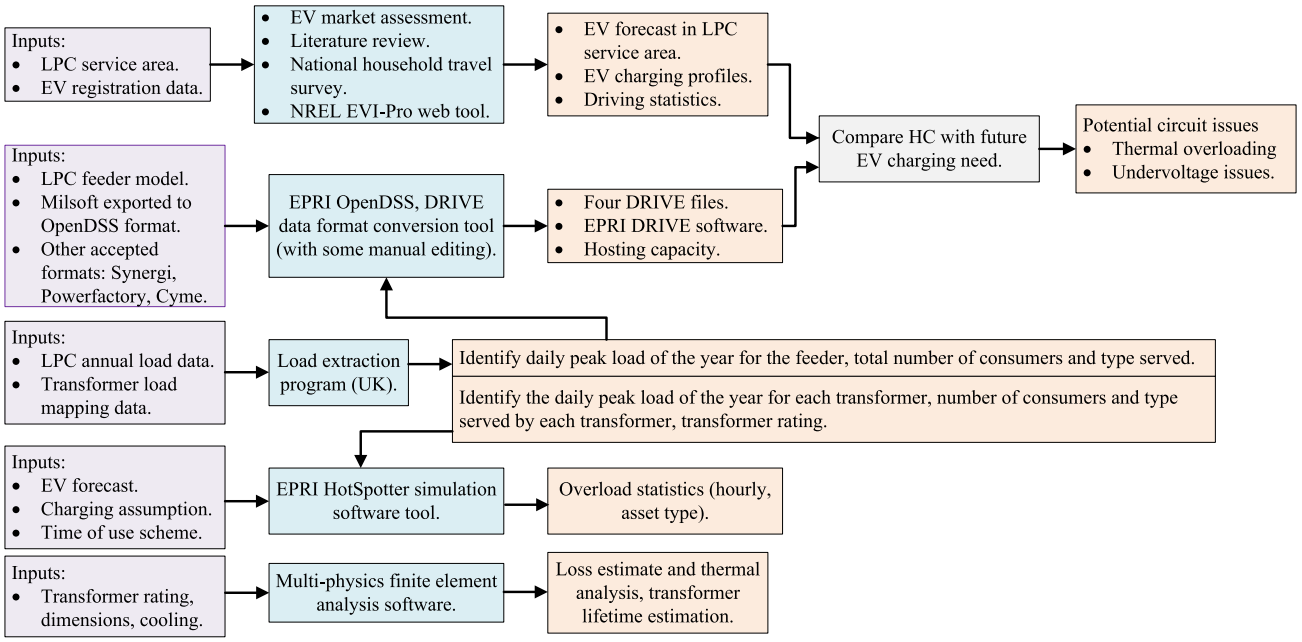

FIGURE 1. Overall analysis flowchart and interdependence of analysis modules.

is why the authors chose to partner with WKRECC for this research. The proposed method and procedure for analyzing EV impacts will be applicable to other power utilities as well.

Fig. 1 depicts the research analysis modules and their relationship and local power company (LPC) data inputs. The first part of this research performs the EV market assessment for the LPC service area to provide EV penetration forecast for the future years under study. The authors also developed a load extraction program to identify the daily peak load of the year and the total number of consumers served by each transformer and by the entire feeders. Then the DRIVE analysis is performed to determine the hosting capacity (HC) of the feeders under study and identify potential problems including undervoltage and thermal overloading issues due to growing EV demand. The Hotspotter analysis identifies the distribution transformer overload statistics by hour and by asset type. The finite element analysis module obtains the loss components estimate (core loss, winding loss density), thermal analysis (hot-spot temperature estimate), and transformer lifetime estimation.

The same analysis procedure can be applied to another LPC. As shown in Fig. 1, the LPC inputs include service area EV registration data, LPC feeder model in Milsoft, OpenDSS, Synergi, Powerfactory, Cyme or other specified format, LPC yearly load data and transformer-load mapping data, and time of use scheme.

The rest of this paper is organized as follows: The Western Kentucky EV market penetration projections and the related load data are presented in Section II. Section III assesses the impacts of EVs on the Western Kentucky distribution system using the DRIVE software tool. The impact of EV charging on the distribution transformer lifetime aging utilizing the HotSpotter and finite element analysis is discussed in Section IV. Finally, technical challenges and potential future research topics are discussed in Section V.

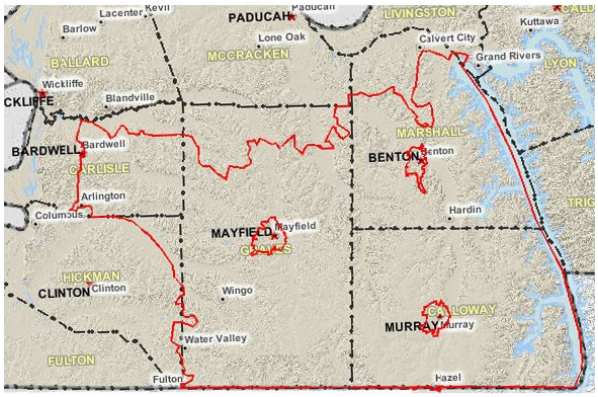

FIGURE 2. West kentucky rural utility grid service area.

II. EV MARKET PROJECTION IN WESTERN KENTUCKY

The West Kentucky Rural Electric Cooperative Corporation is a community-focused electric cooperative established to deliver affordable, reliable, and sustainable energy to more than 31,000 members [23]. Fig. 2 shows the WKRECC service area that consists of Calloway and most of Graves, Carlisle and Marshall Counties. The cooperative has 13 substations at 69 kV and 161 kV, and the distribution system is rated at the 12.5 kV and 25 kV levels.

According to [24], Fig. 3 shows U.S. EV market growth projection in three scenarios, i.e., low, medium and high

TABLE 2. U.S. cumulative EV projections for low, medium and high scenarios [24].

Year	EV fleet size (low)		EV fleet size (medium)		EV fleet size (high)	
	Number in Millions	Market share (%)	Number in Millions	Market share (%)	Number in Millions	Market share (%)
2027	1.5	0.6	10	4	29	12
2030	2.1	0.8	14	5	40	15
2040	5.1	1.7	44	15	113	38
2050	8	2.5	85	26	170	53

TABLE 3. New vehicle registration in Calloway county.

Type	2010	2011	2012	2013	2014	2015	2016	2017	2018	2019	2020	2021
BEV + PHEV new registration	0	1	0	3	3	0	0	3	8	3	4	9
All new registration	898	1001	1049	1059	1151	1108	1142	1079	1092	1001	861	685
% (BEV + PHEV new registration)	0.0	0.1	0.0	0.3	0.3	0.0	0.0	0.3	0.7	0.3	0.5	1.3
BEV + PHEV accumulative	0	1	1	4	7	7	7	10	18	21	25	34
All accumulative	898	1899	2948	4007	5158	6266	7408	8487	9579	**10580**	11441	12126
% (BEV + PHEV accumulative)	0.0	0.0	0.0	0.0	0.1	0.1	0.1	0.1	0.2	0.2	0.2	0.3

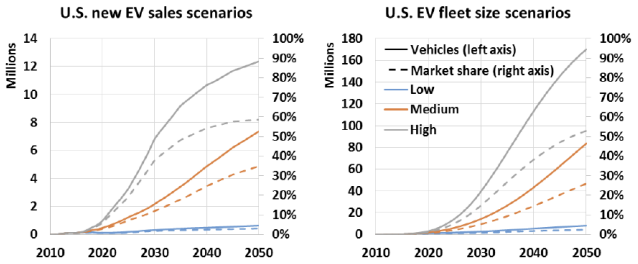

FIGURE 3. EPRI low, medium, high EV market penetration scenarios [24].

scenarios; the number shown is for cumulative EVs in operation. It is seen that the total EV fleet size by 2027 for the three scenarios is forecast to be 1.5 million (0.6% of the total passenger vehicle fleet), 10 million (4%), 29 million (12%), respectively. It is seen that the total EV fleet size by 2030 for the three scenarios is forecast to be 2.1 million (0.8%), 14 million (5%), and 40 million (15%) vehicles, respectively. The EV fleet size by 2040 for the three scenarios is forecast to be 5.1 million (1.7%), 44 million (15%), 113 million (38%), respectively. The EV fleet size by 2050 for the three scenarios is forecast to be 8 million (2.5%), 85 million (26%), 170 million (53%), respectively. Table 2 summarizes the projections under the three scenarios; note that the numbers in the Table 2 are estimated from Fig. 3 since such numeric values are not provided in the reference [24].

A. EV PROJECTION FOR CALLOWAY COUNTY

Since the two feeders under investigation in this study belong to Calloway county, the EV adoption forecast is of particular interest. Table 3 shows the new vehicle registration in Calloway county from 2010 to 2021, according to the data provided by WKRECC. The new PEVs registered each year and accumulative PEVs as well as the percentage of total vehicles is listed. To estimate the accumulative number of vehicles, it is assumed that a vehicle has a service time of 10 years, so the total number of vehicles is about 10,580 in Calloway county, which is used here to calculate the EV share.

It is evinced from Table 3 that EVs account for 0.3% of all vehicles in the county. Looking at the U.S. national EV forecast, we can see that the EV adoption at the Calloway country is in line with the national low-adoption scenario. Even with uncertainty, it is reasonable to believe that the actual EV adoption will fall somewhere between the national low- and medium-adoption scenarios.

B. EV PROJECTION FOR THE MURRAY CITY

One of the representative cities in WRECC's service area is the city of Murray, and this section presents a method for EV projection in Murray. The method presented here is based on the population projection, the average number of vehicles per person, and the assumed EV penetration rate. The method can be applied to other selected areas. If vehicle registration data is available, then the number of vehicles can be used directly.

The number of EVs in a certain region can be estimated by multiplying the population of that region and the count of vehicles per person and the EV penetration rate. Taking the city of Murray as an example, using the penetration rate, the EV projection for the low-, medium- and high-penetration scenarios is shown in Table 4. EV Energy consumption in the city can thus be estimated as follows. Based on the National Survey data, the average vehicle travels 9,579 miles each year. The average EV efficiency of top sold EVs is currently 250.7 Wh/mile [25]. Assume 4.9% system losses for transmission and distribution. Then each EV will consume 2.5 MWh/year of energy. The EV energy consumption projection in city of Murray, KY is provided in Table 5. It should be noted that the above forecast only includes light-duty vehicles. To include the energy consumption of EV buses and trucks, the energy ratio of EV buses and trucks to EV cars shall be used. Accordingly, Table 6 shows the total annual EV energy consumption projection in Murray.

EV power demand profile in a city or area can be estimated using the National Renewable Energy Laboratory (NREL)

TABLE 4. EV projection in city of Murray, KY.

Year	Low	Medium	High
2027	73	484	1,453
2030	98	615	1,844
2040	220	1,941	4,918
2050	341	3,542	7,221

TABLE 5. Annual EV energy consumption projection in city of Murray, KY.

Year	Low (MWh)	Medium (MWh)	High (MWh)
2027	183	1,220	3,659
2030	248	1,548	4,645
2040	554	4,890	12,389
2050	858	8,924	18,191

TABLE 6. Annual EV energy consumption projection in city of Murray, KY including buses and trucks.

Year	Low (MWh)	Medium (MWh)	High (MWh)
2027	246	1,638	4,915
2030	333	2,080	6,239
2040	744	6,568	16,638
2050	1,152	11,985	24,430

Electric Vehicle Infrastructure – Projection (EVI-Pro) Lite. In the NREL EVI-Pro Lite user interface, after choosing the State and City for analysis, the user can change a number of assumptions including number of plug-in EVs in the fleet, average daily miles traveled per vehicle, average ambient temperature, percentage of AEVs among EVs, percentage of Sedan EVs, mix of workplace charging, access to home charging, preference for home charging, home charging strategy, and workplace charging strategy. However, the list of cities in Kentucky available for analysis by the tool does not include the cities in the WKRECC service area. In this study, the following assumptions are made:

- WKRECC follows the U.S. national market share projection. Although the actual market share in WKRECC may very well differ from the national projection, the actual market share will likely fall somewhere between those three scenarios.
- WKRECC follows the U.S. national average driving statistics.

C. EV CHARGING PROFILES

EV daily charging profiles are estimated using the EVI-Pro from the NREL with the following assumptions:

- Average ambient temperature: 68° F.
- Plug-in vehicles that are all electric: 75%.
  1) Mix of workplace charging: 20% level 1 and 80% level 2.
  2) Home charging: 50% level 1 and 50% level 2.
- Charging strategy:
  1) Strategy 1: Charging Home: Immediate - as fast as possible; workplace: Immediate-as fast as possible.

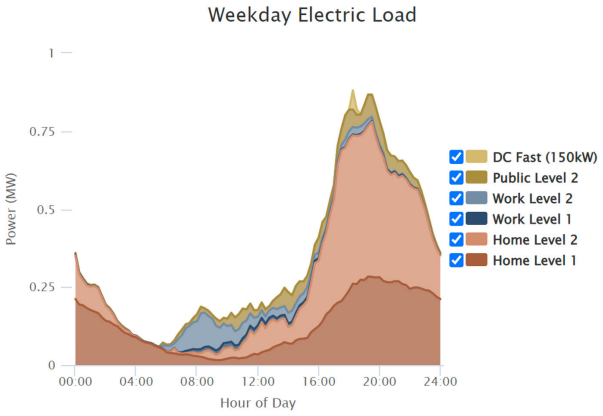

(a) Profile obtained from EVI-Pro tool.

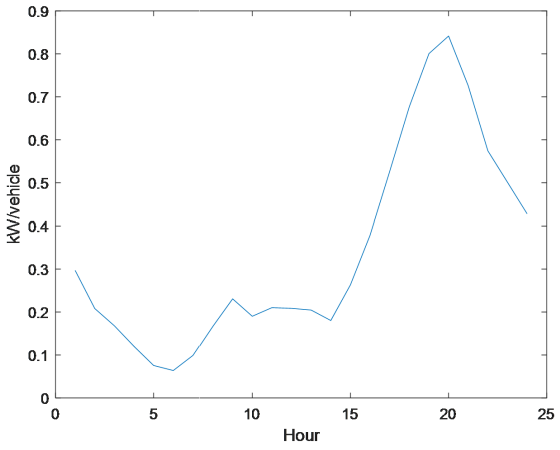

(b) Hourly charging profile per vehicle.

FIGURE 4. EV charging profile, Strategy 1 - Home: immediate-as fast as possible, work: immediate-as fast as possible.

  2) Strategy 2: Home: Immediate - as slow as possible (even spread); workplace: Immediate - as slow as possible (even spread).
  3) Strategy 3: Home: Delayed-finish by departure; workplace: Delayed-finish by departure.
  4) Strategy 4: Home: Delayed-start at midnight; workplace: Delayed-finish by departure.

Using the NREL EVI-PRO tool, the charging profiles for 1000 EVs with the four typical charging strategies listed above are obtained as shown in Fig. 4, Fig. 5, Fig. 6 and Fig. 7. In each figure, sub-figure (a) is the 15-minute charging profile obtained from EVI-Pro tool for 1000 EVs, and sub-figure (b) is the hourly charging profile per vehicle, calculated by averaging the 15-minute power of each hour. The hourly charging profiles corresponding to projected EVs can be obtained by multiplying the projected EV number and the charging profile of sub-figure (b).

Table 7 shows the numeric value of the hourly EV charging demand (kW/vehicle) under the four charging strategies. Under charging strategy 1, the peak charging load is 0.8416 kW/vehicle occurring during the 20th hour of the day.

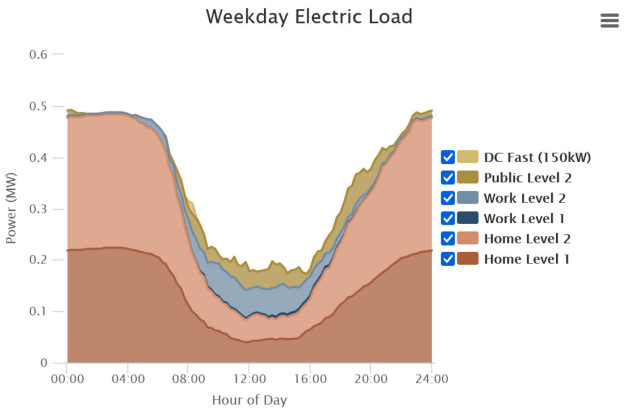

(a) Profile obtained from EVI-Pro tool.

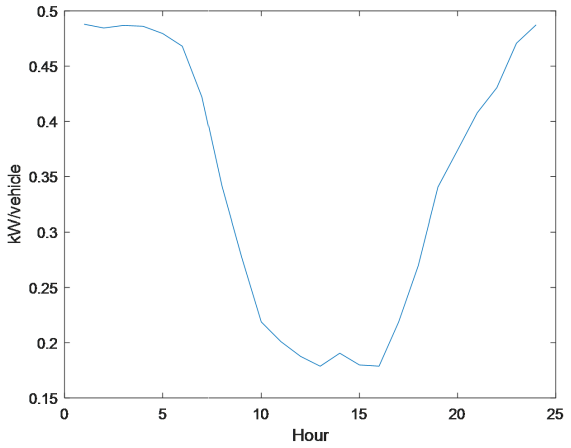

(b) Hourly charging profile per vehicle.

FIGURE 5. EV charging profile, Strategy 2 - Home: immediate-as slow as possible, work: immediate-as slow as possible.

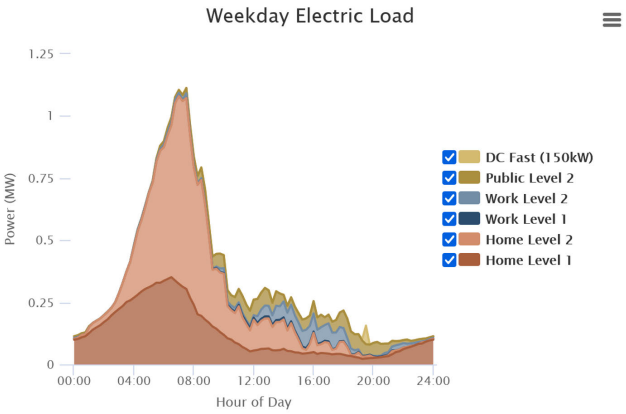

(a) Profile obtained from EVI-Pro tool.

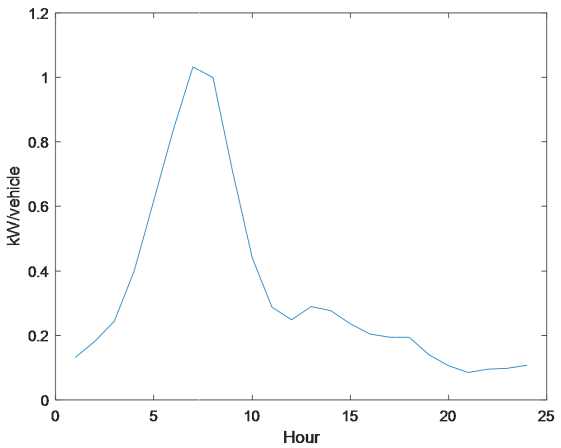

(b) Hourly charging profile per vehicle.

FIGURE 6. EV charging profile, Strategy 3 - Home: delayed-finish by departure, work: delayed-finish by departure.

For strategy 2, the peak charging load is 0.4879 kW/vehicle occurring during the 1st hour of the day. For strategy 3, the peak charging load is 1.0324 kW/vehicle occurring during the 7th hour of the day. Charging strategy 4 has the highest peak load among the four strategies, with a peak of 2.9133 kW/vehicle occurring during the 1st hour of the day.

D. EV ADOPTION PREDICTION FOR THE STUDIED CIRCUITS IN WESTERN KENTUCKY

Two system circuit models, i.e., Circuit STELLA and Circuit E_MURRAY, from the WKRECC are collected to investigate in this study. The residential EV adoption prediction for the two WKRECC circuits is presented as follows. A yearly population increase of 0.52% is assumed. The forecast for the number of residential households and number of EVs served by the two circuits are shown in Table 8 and Table 9, respectively. Column 1 lists the year predicted, Column 2 provides the forecast of the number of residential households, and Column 3 provides the number of estimated vehicles. The last three columns give the forecasted number of EVs for low, medium and high EV adoption scenarios, respectively.

Using the EV charging profiles obtained in the previous section, the peak EV demand for the two circuits are shown in Table 10 and Table 11, respectively. The columns low, medium and high correspond to the three EV prediction scenarios. The column Max represents the maximum peak EV demand assuming a 100% EV adoption.

III. WKRECC CIRCUIT ANALYSIS USING DRIVE

DRIVE software tool is used in this research for evaluating the impacts of adding energy resources including generations, loads and storage devices to a distribution system. DRIVE can be used for both planning and screening. According to [26], planning aims to evaluate the ability of the distribution system to accommodate new resources, which may be distributed at multiple locations, over a period of time such as months to years, without adversely impacting power quality and reliability and without requiring infrastructure upgrades. Screening examines the ability of the distribution system to accommodate a new resource in the near term at a particular location. The ability to add additional load or generation is known as the system's hosting capacity'

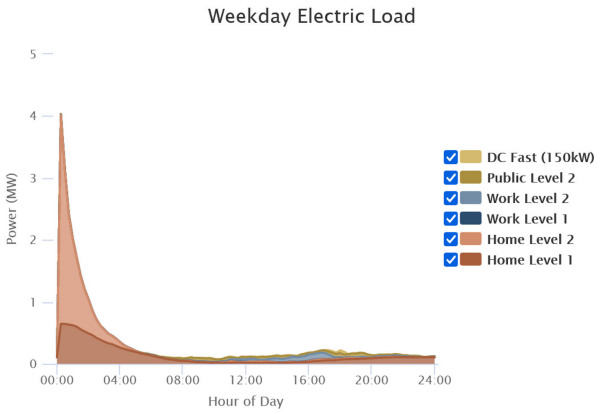

(a) Profile obtained from EVI-Pro tool.

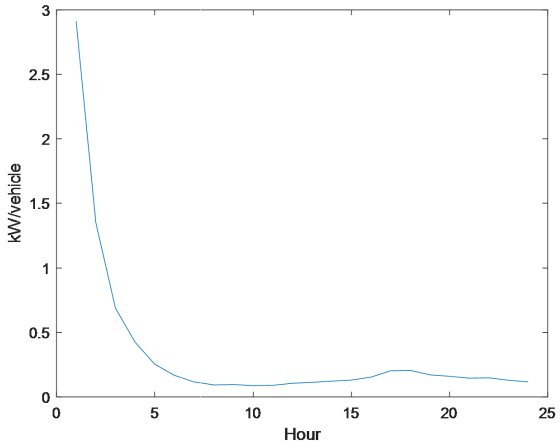

(b) Hourly charging profile per vehicle.

FIGURE 7. EV charging profile, Strategy 4—Home: delayed-start at midnight, work: delayed-finish by departure.

for the specified resource. DRIVE can also identify potential mitigation solutions to increase hosting capacity, identify optimal dispatch/deployment opportunities to maximize hosting capacity and identify how system configuration change affects hosting capacity [27].

This study uses DRIVE to evaluate the capacity of WKRECC circuits [Circuit STELLA and Circuit E_MURRAY] to meet future EV charging needs under assumed EV adoption scenarios. Possible overloading (thermal congestion) on circuit and undervoltage violation are examined. Here, models for two circuit E_MURRAY and STELLA in OpenDSS files were collected where the WKRECC load data obtained at various consumer locations were summarized. In circuit STELLA, the peak load is 5.2 MW, which occurred at 6 PM on August 11, 2021. The minimum load on that day is 2.04 MW. The corresponding daily load profile is shown in Fig. 8. The horizontal axis represents the hour from the first hour in the morning to the last hour at the night of the day. In circuit E_MURRAY, the peak load is 5.68 MW, which occurred at 12 PM on February 15, 2021. The minimum load on that day is 4.7 MW. The corresponding daily load profile is shown in Fig. 9.

TABLE 7. EV charging profiles (kW/vehicle) for the four charging strategies.

Hour	EV charging demand (kW)			
	Charging strategy 1	Charging strategy 2	Charging strategy 3	Charging strategy 4
1	0.297	**0.4879**	0.1315	**2.9133**
2	0.2082	0.4845	0.1818	0.1352
3	0.1679	0.4868	0.2447	0.6899
4	0.1201	0.4861	0.3991	0.4255
5	0.0756	0.4795	0.6163	0.2549
6	0.0639	0.468	0.8371	0.168
7	0.0989	0.4219	**1.0324**	0.1168
8	0.1671	0.3414	0.9991	0.0932
9	0.2307	0.2776	0.707	0.0962
10	0.1902	0.2188	0.4414	0.0875
11	0.2102	0.201	0.2882	0.0902
12	0.2086	0.1877	0.2488	0.106
13	0.2046	0.1787	0.2898	0.1132
14	0.1803	0.1905	0.2771	0.1227
15	0.2633	0.1799	0.2363	0.131
16	0.3787	0.1788	0.2044	0.1541
17	0.5264	0.2189	0.1948	0.2031
18	0.677	0.2699	0.1942	0.2057
19	0.8006	0.3406	0.1403	0.1715
20	**0.8416**	0.374	0.1061	0.1602
21	0.7258	0.4077	0.0853	0.1458
22	0.5743	0.4305	0.0955	0.1483
23	0.5011	0.4708	0.0983	0.1297
24	0.4276	0.4874	0.1076	0.1167

TABLE 8. Residential EV adoption prediction for circuit STELLA.

Year	Residential	Vehicle	EV (low)	EV (medium)	EV (high)
2027	1076	1998	12	80	240
2030	1092	2030	16	101	304
2040	1151	2138	36	321	812
2050	1212	2252	56	585	1193

A. ANALYSIS FOR STELLA CIRCUIT MODEL

Using the OpenDSS software tool, Circuit STELLA is plotted and shown in Fig. 10, where the thickness of the line is proportional to the real power on the line.

Fig. 11 shows the centralized HC analysis results for circuit STELLA. It is seen that the maximum HC capacity is 1.4 MW, 1.3 MW and 4.3 MW without causing feeder thermal, primary undervoltage and voltage deviation problems, respectively. The locations of the circuit to place load, which may cause potential problems, are downstream circuits that are further away from the feederhead.

Choosing option 'Full' for distributed resource location and 1Non-uniform' for distributed resource distribution, Fig. 12 depicts the distributed HC analysis results for circuit STELLA. The results indicate that the feeder can host 3.7 MW additional load without causing undervoltage problems, 2.7 MW additional load without causing thermal problems, and 15.0 MW additional load without causing voltage deviation problems.

Choosing option 'Full' for distributed resource location and 'Uniform' for distributed resource distribution, Fig. 13 depicts the distributed HC analysis results for circuit STELLA. The results indicate that the feeder can host

TABLE 9. Residential EV adoption prediction for circuit E_MURRAY.

Year	Residential	Vehicle	EV (low)	EV (medium)	EV (high)
2027	1432	2660	16	106	319
2030	1454	2702	22	135	405
2040	1532	2846	48	427	1081
2050	1613	2997	75	779	1588

5.5 MW additional load without causing undervoltage problems, 5.6 MW additional load without causing thermal problems, and 15.0 MW additional load without causing voltage deviation problems.

Choosing option 1At Existing Loads' for distributed resource location and 1Non-Uniform' for distributed resource distribution, Fig. 14 depicts the distributed HC analysis results for circuit STELLA. In this option, the future load is allocated at existing loads and the amount of allocation is proportional to the existing loads. The results indicate that the feeder can host 4.0 MW additional load without causing undervoltage problems, 3.5 MW additional load without causing thermal problems, and 15.0 MW additional load without causing voltage deviation problems.

Choosing option 1At Existing Loads' for distributed resource location and 'Uniform' for distributed resource distribution, Fig. 15 depicts the distributed HC analysis results for circuit STELLA. In this option, the future load is allocated at existing loads and the amount of allocation is uniform across the existing loads. The results indicate that the feeder can host 3.9 MW additional load without causing undervoltage problems, 3.5 MW additional load without causing thermal problems, and 15.0 MW additional load without causing voltage deviation problems.

Table 12 provides a summary of the hosting capacity results for circuit STELLA. The 2nd, 3rd and 4th columns indicate the hosting capacity without causing problems for undervoltage, thermal overloading and voltage deviation criterion, respectively. The smallest number will be the limiting factor for hosting future load growth.

The ability of circuit STELLA to meet future EV charging needs is analyzed as follows. Referring to the EV demand prediction as shown in Table 8, it can be seen that assuming centralized charging integration, the circuit STELLA has no problem to meet the forecasted EV demand under the low, medium and high EV adoption scenarios from now to the year of 2050 for EV charging strategy 1-3. For charging strategy 4, the peak EV demand is 3.48 MW in the high EV adoption scenario, which is much larger than the centralized HC of 1.3 MW. Although it is unlikely that all the EVs will be charged at a single location, centralized HC tells us the potential ability of the circuit to charge future EVs at a single location, which may provide guidance for planning big charging stations.

For all the four distributed charging integration options except 'Distributed-Full, Non-uniform', the circuit STELLA can meet the forecasted EV demand without any problem for the three EV adoption scenarios for the four charging strategies. Even for the assumed 100% EV adoption scenario, no issue is expected for charging strategy 1, 2 and 3 with each of the four distributed charging integration options.

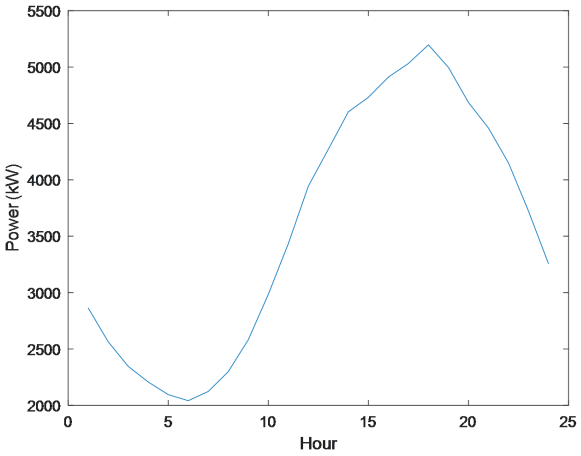

FIGURE 8. Daily peak load profile for Circuit STELLA.

The charging integration option of 'Distributed-At Existing loads, either Non-uniform or uniform' seems a reasonable assumption for future residential households.

It is noted that the HC shown in Table 12 corresponds to the peak load of the circuit, since the peak EV charging demand may not coincide with the peak load, Table 12 provides a conservative estimate of HC. In other words, the HC of the circuit would be larger than the values shown in Table 12 in cases where the peak load of the circuit and EV charging demand peak do not occur at the same time. For Circuit STELLA, the peak load is in the afternoon, which is close to the EV charging demand peak time of charging strategy 1, but is distant from the EV charging demand peak time of charging strategy 2, 3 and 4 that is in the morning or around the midnight.

In cases where the HC of the circuit at each load level of the daily profile shown in Fig. 8 is desired or needed, the function 1Time-Series Hosting Capacity (TSHC)' of DRIVE tool can be used to achieve this. Fig. 16 depicts the hosting capacity for STELLA using the daily peak load profile. It is seen that the HC is minimum at the peak load and is larger at other times and can be quite high at light load conditions. The thermal constraint is the limiting factor for EV adoption for circuit STELLA.

Fig. 17 depicts the TSHC with 'Distributed-At Existing loads, Non-uniform' and the four EV charging profiles under high EV adoption scenario in 2050. Fig. 18 depicts the 100% EV adoption scenario in 2050. It clearly indicates that circuit STELLA has no problem in hosting future EVs under the high EV adoption scenario, but has issues for 100% EV adoption scenario under charging strategy 4.

The thermal hosting capacity decreases when the ambient temperature of the feeders increases. The derated thermal HC (TLHC) and four charging profiles are shown in Fig. 19 and Fig. 20 for high EV adoption and 100% adoption in 2050.

TABLE 10. Circuit STELLA peak EV demand prediction.

	Peak EV demand kW (Charging strategy 1)				Peak EV demand kW (Charging strategy 2)				Peak EV demand kW (Charging strategy 3)				Peak EV demand kW (Charging strategy 4)			
Year	Low	Medium	High	Max	Low	Medium	High	Max	Low	Medium	High	Max	Low	Medium	High	Max
2027	10	67	201	1681	5	39	117	974	12	82	247	2063	34	232	698	5821
2030	13	85	256	1708	7	49	148	990	16	104	314	2095	47	295	886	5913
2040	30	269	683	1799	17	156	396	1043	37	331	838	2206	105	934	2366	6227
2050	47	492	1004	1894	27	285	582	1098	58	604	1231	2324	163	1705	3476	6559

TABLE 11. Circuit E_MURRAY peak EV demand prediction.

	Peak EV demand kW (Charging strategy 1)				Peak EV demand kW (Charging strategy 2)				Peak EV demand kW (Charging strategy 3)				Peak EV demand kW (Charging strategy 4)			
Year	Low	Medium	High	Max	Low	Medium	High	Max	Low	Medium	High	Max	Low	Medium	High	Max
2027	13	89	268	2238	7	51	155	1297	16	109	329	2746	46	309	929	7749
2030	18	113	341	2273	10	65	197	1318	22	139	418	2789	62	393	1180	7870
2040	40	359	910	2394	23	208	527	1388	49	440	1116	2937	140	1243	3150	8289
2050	63	655	1336	2522	36	380	774	1462	77	804	1639	3094	218	2270	4627	8731

TABLE 12. Summary of hosting capacity results for circuit STELLA.

Analysis option	Hosting capacity (MW)		
	Primary under voltage	Thermal	Primary voltage deviation
Centralized	1.4	1.3	4.3
Distributed-Full, Non-uniform	3.7	2.7	15
Distributed-Full, uniform	5.5	5.6	15
Distributed-At Existing loads, Non-uniform	4	3.5	15
Distributed-At Existing loads, uniform	3.9	3.5	15

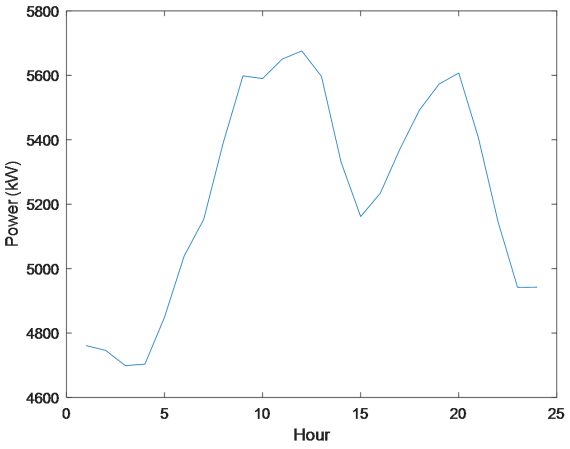

FIGURE 9. Daily peak load profile for Circuit E_MURRAY.

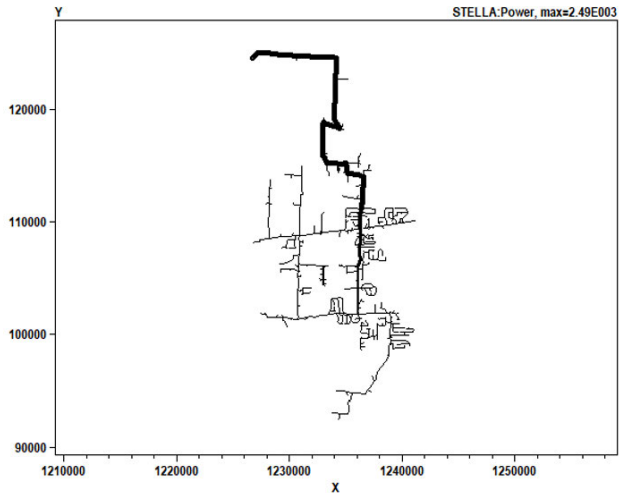

FIGURE 10. Plot of Circuit STELLA.

Here, 'CS' represents Charging Strategy. The 'TLHC-90%' is the TLHC calculated assuming that the circuit thermal capacity is 90% of the originally rated capacity of the circuit. The original rating is specified at 77 Fahrenheit ambient temperature and 2 ft/second wind speed. The 50% rating is usually used in utilities for 100 Fahrenheit ambient temperature and 0 ft/second wind speed. The TLHC-100% is obtained by DRIVE tool using the originally rated circuit model. Derated TLHC is obtained as follows: the TLHC-100% + Load is regarded as the original thermal capacity of the circuit, which is multiplied by the derating factor say 90% to yield the derated thermal capacity. The derated thermal capacity minus the load gives the TLHC-90%.

In high EV adoption scenario, a thermal capacity derating of 70% would cause thermal problems for charging strategy 4. In 100% adoption scenario, a derating of 70% would cause thermal problems for charging strategy 1 in addition to CS4.

It is recognized that the TSHC results obtained here utilize the daily peak load in 2021. Future load increase may include not only EVs but also other non-EV loads. The non-EV load will certainly affect the ability of a power system to host EVs. Therefore, the forecast for non-EV loads for the future, if available, should be considered in the process of EV adoption analysis.

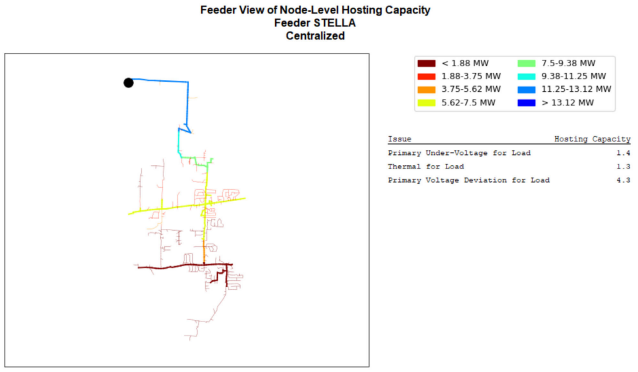

FIGURE 11. Centralized HC analysis results for STELLA.

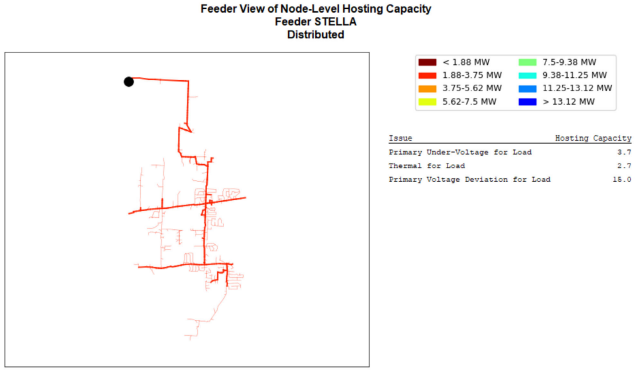

FIGURE 12. Distributed HC analysis results for STELLA-Full, Non-uniform.

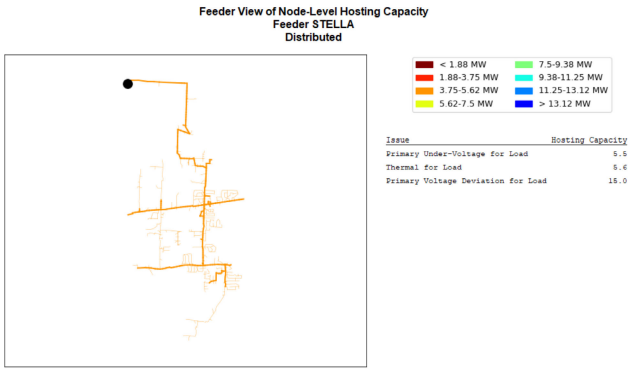

FIGURE 13. Distributed HC analysis results for STELLA – Full, Uniform.

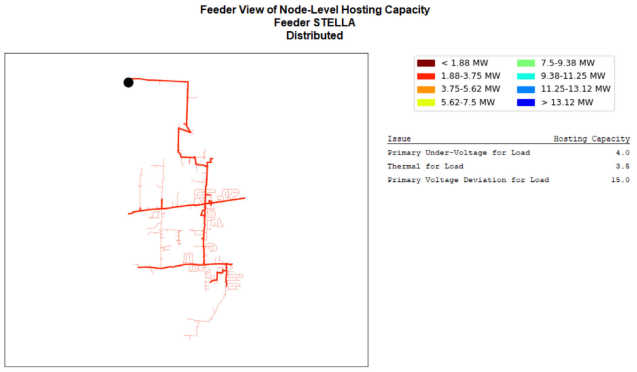

FIGURE 14. Distributed HC analysis results for STELLA – At Existing Loads, Non-Uniform.

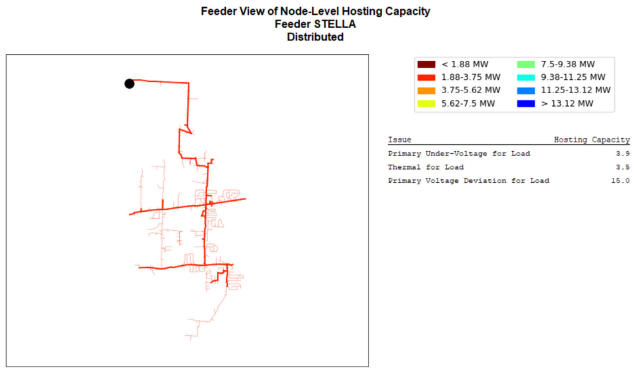

FIGURE 15. Distributed HC analysis results for STELLA – At Existing Loads, Uniform.

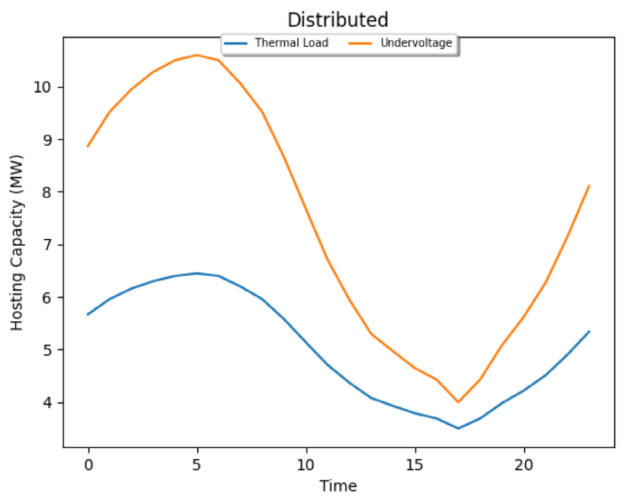

FIGURE 16. TSHC for STELLA, distributed-at existing loads, Non-uniform.

B. ANALYSIS FOR E_MURRAY CIRCUIT MODEL

Using the OpenDSS software tool, Circuit E_MURRAY is visually plotted in Fig. 21, where the thickness of the line is proportional to the real power on the line.

The DRIVE hosting capacity analysis is presented as follows. Fig. 22 shows the centralized HC analysis results for circuit E_MURRAY. It is seen that the maximum HC capacity is 1.7 MW, 1.0 MW and 3.0 MW without causing feeder thermal, primary undervoltage and voltage deviation problems, respectively. The locations of the circuit to place load, which may cause potential problems, are downstream circuits that are further away from the feederhead.

Choosing option 'Full' for distributed resource location and 'Non-uniform' for distributed resource distribution, Fig. 23 depicts the distributed HC analysis results for circuit E_MURRAY. The results indicate that the feeder can

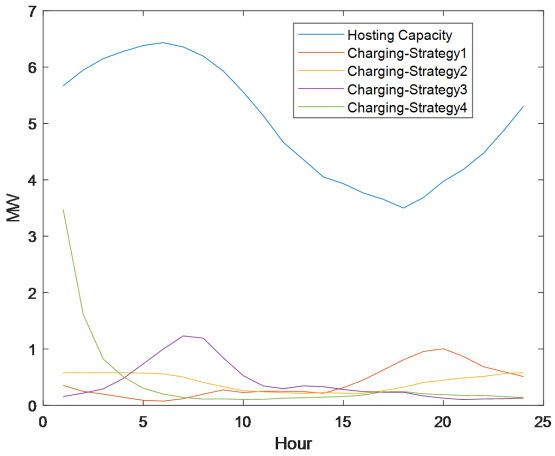

FIGURE 17. STELLA TSHC and EV charging profiles under the four charging strategies, High EV adoption scenario in 2050.

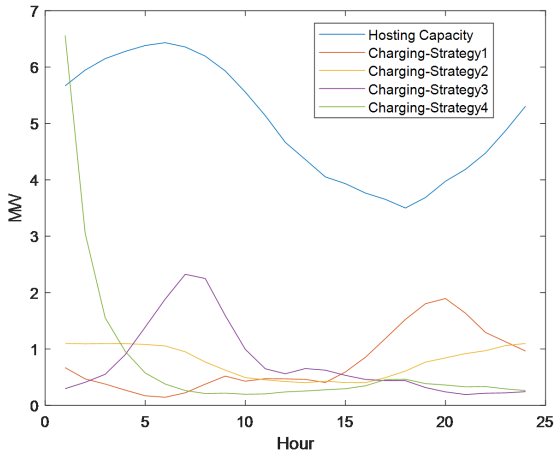

FIGURE 18. STELLA TSHC and EV charging profiles under the four charging strategies, 100% EV adoption scenario in 2050.

host 4.5 MW additional load without causing undervoltage problems, 5.7 MW additional load without causing thermal problems, and 15.0 MW additional load without causing voltage deviation problems.

Choosing option 'Full' for distributed resource location and 'Uniform' for distributed resource distribution, Fig. 24 depicts the distributed HC analysis results for circuit E_MURRAY. The results indicate that the feeder can host 6.7 MW additional load without causing undervoltage problems, 11.5 MW additional load without causing thermal problems, and 15.0 MW additional load without causing voltage deviation problems.

Choosing option 'At Existing Loads' for distributed resource location and 'Non-Uniform' for distributed resource distribution, Fig. 25 depicts the distributed HC analysis results for circuit E_MURRAY. In this option, the future load is allocated at existing loads and the amount of allocation is proportional to the existing loads. The results indicate that the feeder can host 5.3 MW

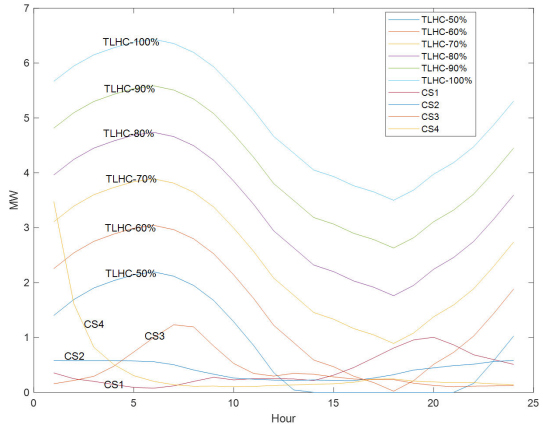

FIGURE 19. STELLA UVHC, TLHC with various derating percentages, and EV charging profiles, High EV adoption scenario in 2050.

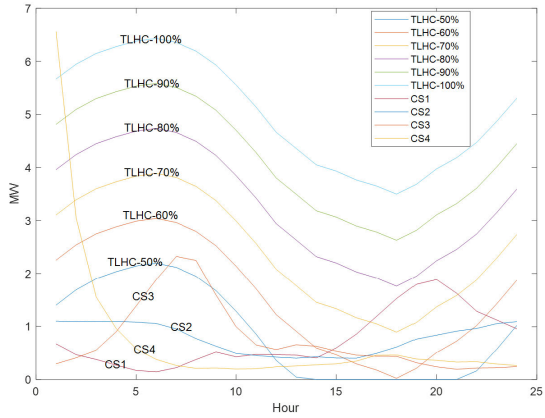

FIGURE 20. STELLA UVHC, TLHC with different derating percentages, and EV charging profiles, 100% EV adoption scenario in 2050.

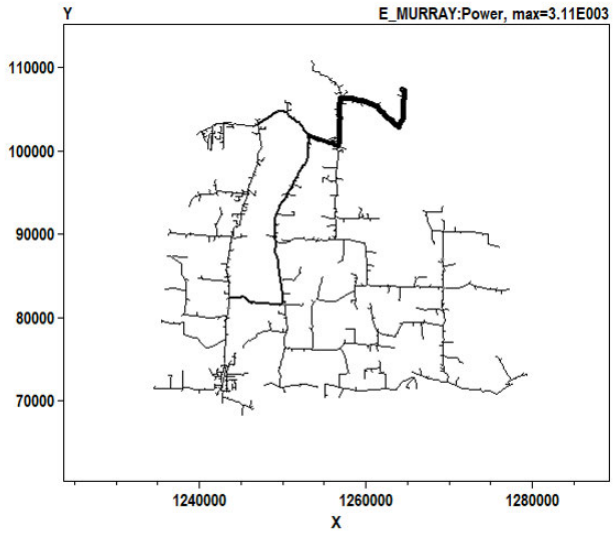

FIGURE 21. Plot of Circuit E_MURRAY.

additional load without causing undervoltage problems, 6.9 MW additional load without causing thermal problems,

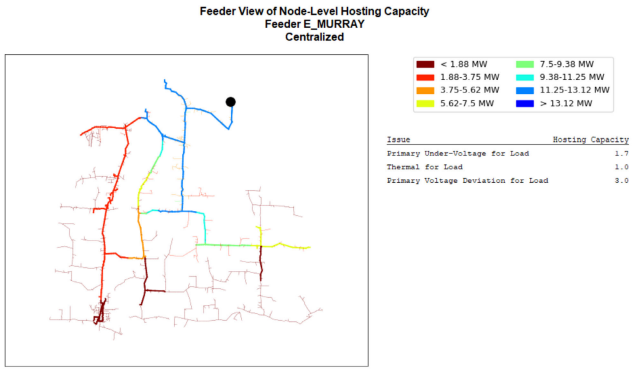

FIGURE 22. Centralized HC analysis results for E_MURRAY.

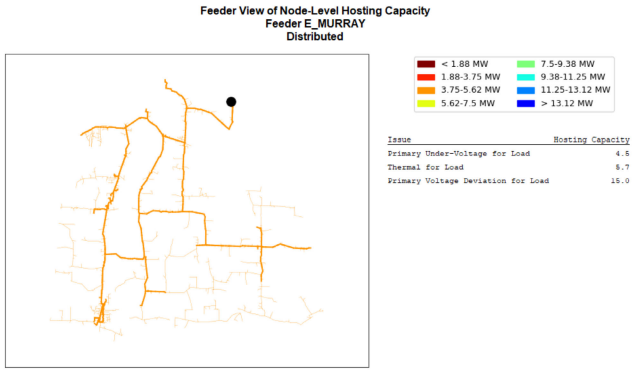

FIGURE 23. Distributed HC analysis results for E_MURRAY-Full, Non-uniform.

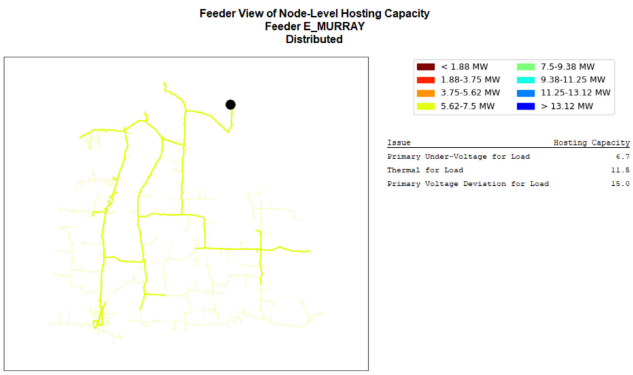

FIGURE 24. Distributed HC analysis results for E_MURRAY-Full, Uniform.

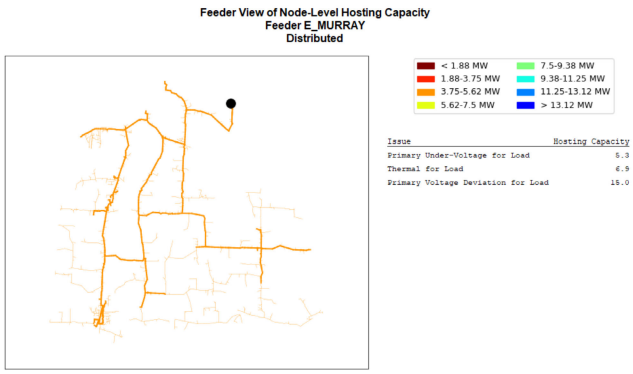

FIGURE 25. Distributed HC analysis results for E_MURRAY-At Existing Loads, Non-Uniform.

and 15.0 MW additional load without causing voltage deviation problems.

Choosing option 'At Existing Loads' for distributed resource location and 'Uniform' for distributed resource distribution, Fig. 26 depicts the distributed HC analysis results for circuit STELLA. In this option, the future load is allocated at existing loads and the amount of allocation is uniform across the existing loads. The results indicate that the feeder can host 5.2 MW additional load without causing undervoltage problems, 7.2 MW additional load without causing thermal problems, and 15.0 MW additional load without causing voltage deviation problems.

Table 13 provides a summary of the hosting capacity results for circuit E_MURRAY. The 2nd, 3rd and 4th columns indicate the hosting capacity without causing problems for undervoltage, thermal overloading and voltage deviation criterion, respectively.

The ability of circuit E_MURRAY to meet future EV charging needs is analyzed as follows. With centralized charging integration, referring to the EV demand prediction as shown in Table 9, it can be seen that the circuit E_MURRAY has no problem to meet the forecasted EV demand from now to the year of 2040 for EV charging strategy 1 and 3, from now to 2050 for charging strategy 2, and from now to about 2030 for charging strategy 4.

For distributed charging integration, the circuit E_MURRAY can meet the forecasted EV demand without any problem for the three EV adoption scenarios under the four charging strategies, except the option 'Distributed-Full, Non-uniform' has a HC of 4.5 MW due to undervoltage issue which is slightly lower than 4.6M in high EV adoption scenario with charging strategy 4. Even for the assumed 100% EV adoption scenario, no issue is expected from now to 2050 for charging strategies 1 to 3.

A time-series hosting capacity analysis is performed using the option 'Distributed-At Existing loads, Non-uniform', and the results are shown in Fig. 27. It is evinced that the HC is minimum at the peak load and is much higher at light load conditions. It is also shown that the undervoltage HC is the constraining HC.

Fig. 28 depicts the TSHC and the four EV charging profiles under high EV adoption scenario in 2050. Fig. 29 depicts the 100% EV adoption scenario in 2050. It clearly indicates that circuit E_MURRAY has no problem in hosting future EVs under high EV adoption scenario but has issues for 100% EV adoption scenario under charging strategy 4.

The thermal hosting capacity decreases when the ambient temperature of the feeders increases. The UVHC, derated thermal HC (TLHC) and four charging profiles are shown in Fig. 30 and Fig. 31 for high EV adoption and 100% adoption

TABLE 13. Summary of hosting capacity results for circuit E_MURRAY.

Analysis option	Hosting capacity (MW)		
	Primary under voltage	Thermal	Primary voltage deviation
Centralized	1.7	1	3
Distributed-Full, Non-uniform	4.5	5.7	15
Distributed-Full, uniform	6.7	11.5	15
Distributed-At Existing loads, Non-uniform	5.3	6.9	15
Distributed-At Existing loads, uniform	5.2	7.2	15

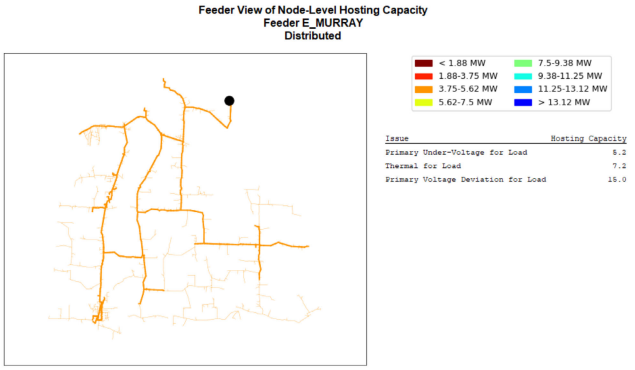

FIGURE 26. Distributed HC analysis results for E_MURRAY-At Existing Loads, Uniform.

in 2050. In Fig. 30 and Fig. 31, 'CS' represents Charging Strategy. In high EV adoption scenario, a thermal capacity derating of 70% would cause thermal problems for charging strategy 4. In 100% adoption scenario, a derating of 60% would cause thermal problems for charging strategy 1 and 3 in addition to CS4.

As discussed for the circuit STELLA, it should be pointed out here that the forecast for non-EV loads for the future, if available, should be considered in the process of EV adoption analysis.

IV. IMPACTS OF EV CHARING ON THE RELIABILITY OF DISTRIBUTION TRANSFORMERS

In this section, the impact of EV intensive charging on the lifetime degradation of distribution transformers has been investigated. The HotSpotter software tool based on a probabilistic method is employed to assess the system-wide impact of EV charging on residential distribution transformers. In addition, the authors also studied the overload and aging impact of EV charging by conducting finite element analysis of a distribution transformer.

A. HotSpotter ANALYSIS

HotSpotter is a software tool developed by EPRI that utilities can use to pinpoint the most vulnerable customer service transformers, which helps the utilities prioritize and manage the EV charging to ensure the grid reliability. By analyzing EV adoption rates, charging time and rates, and other EV data, HotSpotter simulates load impacts on a transformer based on its nameplate rating, peak load, the number of customers it serves, and other characteristics [28].

Here, the input of the HotSpotter tool includes the transformer data as well as the parameters and assumptions of the EV charging. HotSpotter carries out the computation for 2025 and 2035, targeting at both low and high EV penetration as well as managed and unmanaged scenarios. Here, managed charging refers to the restricted charging for certain hours, and unmanaged charging refers to no restrictions for charging hours. Fig. 32 shows the flowchart of the HotSpotter analysis.

1) HotSpotter DATA INPUT PREPARATION

The distribution transformer asset data and raw load data are collected from the WKRECC in excel sheet format for the year 2021. Then the authors developed MATLAB scripts to extract the transformer data, including transformer rating, number of consumers and consumer type, and daily peak load for HotSpotter analysis. The consumer type includes residential, small commercial, large commercial, and large power. When performing HotSpotter analysis, only residential-type consumers are considered.

2) ASSET DATA OVERVIEW

The total number of distribution transformers provided by WKRECC is 1,659, while the number of the analyzed distribution transformers with compatible data is 1,153. Depending on the projected year (2025 and 2035), penetration level, and management, there are 8 scenarios investigated in this task, as shown in Table 14. The percentage of the distribution transformers with different power ratings is shown in Fig. 33(a), and the average number of residents per asset is shown in Fig. 33(b). As can be seen, the transformers with the power ratings of 15 kVA, 25 kVA, and 50 kVA, are the most utilized transformers with a total percentage of 94.9%. Also, the general trend is that, the larger the transformer power ratings, the more residents per asset. For instance, the 100 kVA transformer has 13 residents per asset, much higher than other transformers with lower power ratings.

3) EV AND CHARGING ASSUMPTIONS

Based on four counties served by WKRECC, namely, Calloway, Carlisle, Graves, and Marshall, the projected EV adoption levels for 2025 and 2035 are assumed, as shown in Table 15. Also, the EV fleet size (i.e., the number of vehicles in service) and the EVs per household probabilities are assumed, as shown in Table 16 and Table 17.

The total projected EV penetration over the next 30 years (up to 2050) is shown in Fig. 34, and the EV charger power

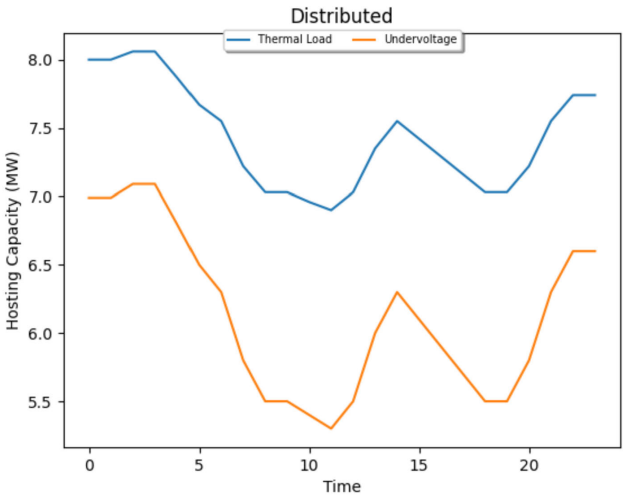

FIGURE 27. TSHC for E_MURRAY, Distributed-At Existing loads, Non-uniform.

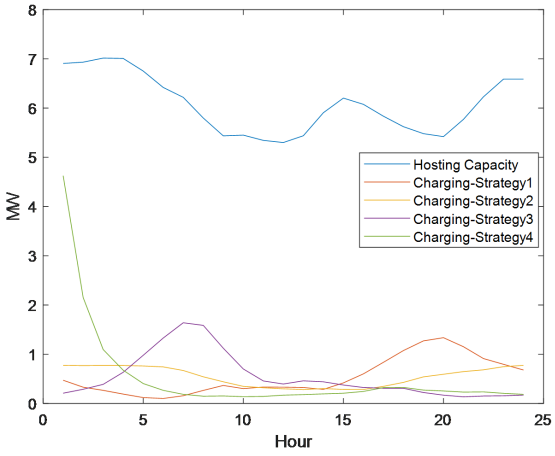

FIGURE 28. E_MURRAY TSHC and EV charging profiles under the four charging strategies, High EV adoption scenario in 2050.

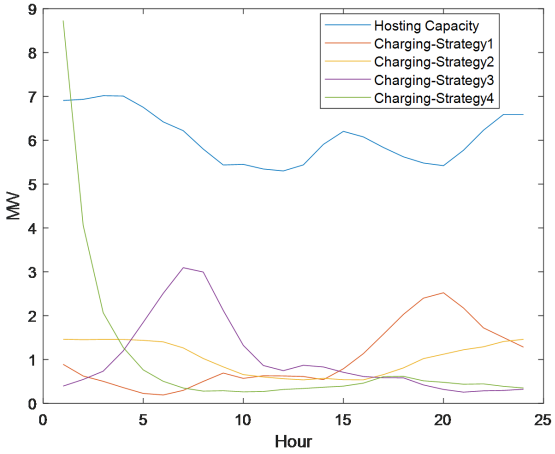

FIGURE 29. E_MURRAY TSHC and EV charging profiles under the four charging strategies, 100% EV adoption scenario in 2050.

ratings along with the EV percentages in zone is shown in Table 18. As can be seen, 7.2 kW battery EVs (BEVs) has the

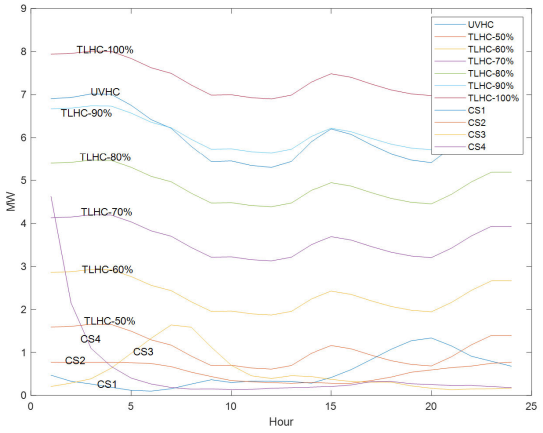

FIGURE 30. E_MURRAY UVHC, TLHC under various derating percentages, and EV charging profiles, High EV adoption scenario in 2050.

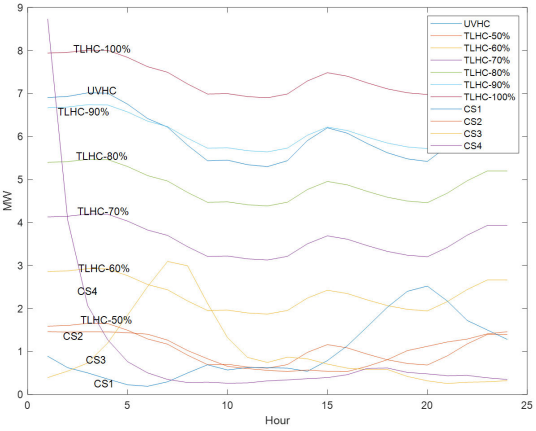

FIGURE 31. E_MURRAY UVHC, TLHC under various derating percentages, and EV charging profiles, 100% EV adoption scenario in 2050.

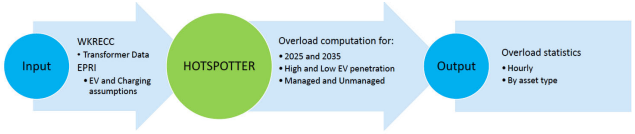

FIGURE 32. Flowchart of the HotSpotter analysis.

TABLE 14. Various scenarios to be analyzed by the HotSpotter tool.

Scenario	Year	EV penetration	Management
1	2025	High	Unmanaged
2	2025	Low	Unmanaged
3	2035	High	Unmanaged
4	2035	Low	Unmanaged
5	2025	High	Managed
6	2025	Low	Managed
7	2035	High	Managed
8	2035	Low	Managed

highest percentage (i.e., 36%) of EVs in zone. Additionally, the customer charging behavior is modeled as a joint probability of miles driven and home arrival time, as shown in

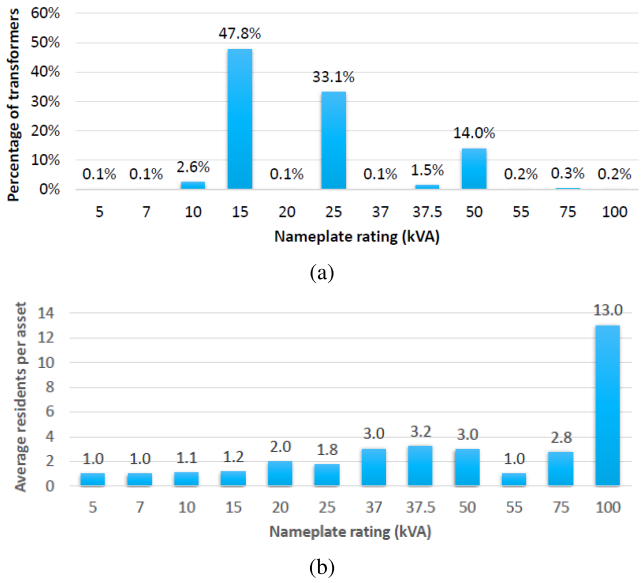

FIGURE 33. Transformer data vs. nameplate ratings (a) percentage of transformers (b) average residents per asset.

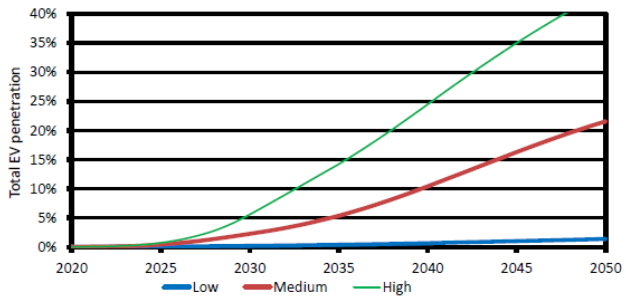

FIGURE 34. Total projected EV penetration over the next 30 year.

TABLE 15. Assumption of the EV penetration level.

Year	Low (%)	High (%)
2025	0.1	0.7
2035	0.4	14.2

TABLE 16. EV fleet size (number of vehicles in service).

Year	Low	High
2025	90	743
2035	402	14,531

Fig. 35. This model assumes charging only once per day and vehicles fully charged each day. Also, the managed charging refers to no charging between 1:00 PM and 6:00 PM each day and restart charging at 6:00 PM.

4) ASSET OVERLOAD OUTPUT IN HotSpotter

The 90th percentile of the number of transformer overload by hours under the managed and unmanaged EV charging

TABLE 17. EVs per household probabilities.

0	1	2
3.8 %	28.8 %	67.4 %

TABLE 18. Various EV charger power ratings and the percentage of EVs in zone.

EV type	Comments	% of EV in zone
2.8 kW PHEV	Toyota Prius Plug in	8.8 %
3.3 kW PHEV	Chevy Volt and Cadillac ELR	10.3 %
3.8 kW PHEV	Ford C-Max and Fusion Energi	15.2 %
7.2 kW BEV	Mainstream BEV	36 %
9.6 kW BEV	Toyota RAV 4 + Tesla Base L2	14.9 %
19.2 kW BEV	Tesla wall charger	14.8 %

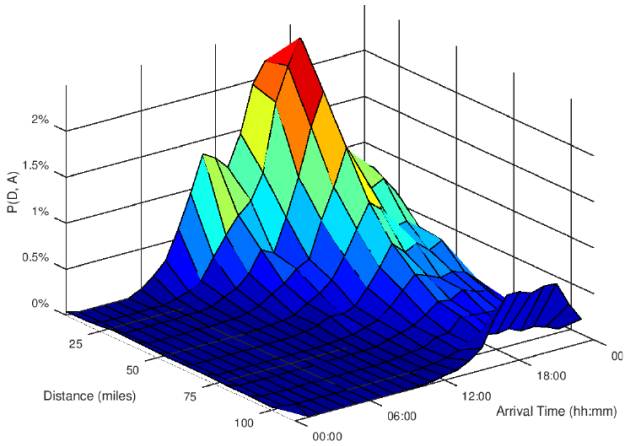

FIGURE 35. Customers' charging probability function vs. miles driven and home arrival time.

scenarios are simulated and shown in Fig. 36, for both 2025 and 2035 projected low and high EV penetration levels. As can be seen that, with the managed EV charging, the number of overloads is significantly reduced during the 13th and 18th hours, but is drastically increased in the 19th and 20th hours following the end of the time-of-use (TOU) scheme. Fig. 37 shows the 90th percentile of projected overloads by transformer ratings under unmanaged and managed EV charging scenarios for 2025 and 2035. As is shown, the largest number of overloads occur for 15 kVA transformers, followed by 10 kVA and then 25 kVA ones.

As pointed out, a high number of overloads occurred immediately after the managed time (13 PM-18 PM) is over. This is due to customers immediately charging after this time period. This indicates that it is essential to design appropriate TOU schemes in order to incentivize consumers to spread the EV charging as much as possible to avoid transformer overloads. Options to avoid such overloading include: (1) actively managed charging to fill the entire time period that the car is parked; (2) programming charging to stop at the end of the charge window- thus shifting charging later; (3) have multiple TOU options so that the drivers spread across multiple charge start times.

TABLE 19. Various EV charger power ratings and the percentage of EVs in zone.

	Charging Management	Hours Controlled	Incentive	Charging Behavior
1	Unmanaged	None	N/A	N/A
2	Managed	1 pm to 6 pm	N/A	Consumer start charging immediately after managed time is over.
3	Managed-Distributed	1 pm to 6 pm	N/A	Charging distributed proportionally during non controlled hours.
4	Managed-Night encouraged	6 pm to 12 am	Night encouraged	80 % at night (12 am to 6 am), 20 % other hours (6 am to 6 pm).

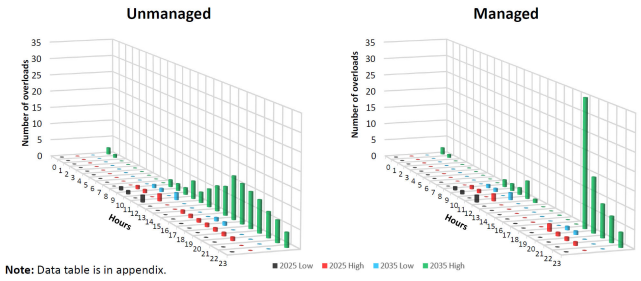

FIGURE 36. Customerscharging probability function vs. miles driven and home arrival time.

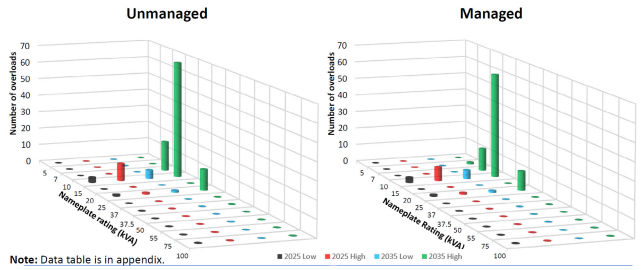

(a) Number of overloads by transformer rating.

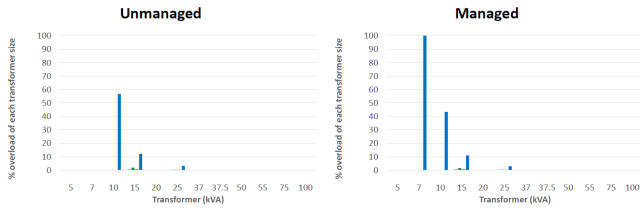

(b) Percentage of overloads by transformer rating.

FIGURE 37. The 90th percentile of projected overloads by transformer ratings under unmanaged and managed EV charging scenarios for 2025 and 2035.

It is seen from Fig. 37 (b) that 56.7% of 10 kVA transformers, 12.2% of 15 kVA transformers, and 3.1% of 25 kVA transformers have overloading for 2035 High scenario for unmanaged case. For managed case, 100% 7 kVA transformers, 43.3% of 10 kVA transformers, 10.9% of 15 kVA transformers, and 2.9% of 25 kVA transformers have overloading for 2035 High scenario.

5) ALTERNATIVE TOU ASSUMPTIONS AND OUTPUT OVERLOAD

Impact of EV charging on transformers with alternative TOU assumptions was also investigated. As shown in Table 19, two alternative TOU assumptions were made, one is charging distributed proportionally during non-controlled hours, and another is 80% at night (12 AM-6 PM) and 20% for daytime

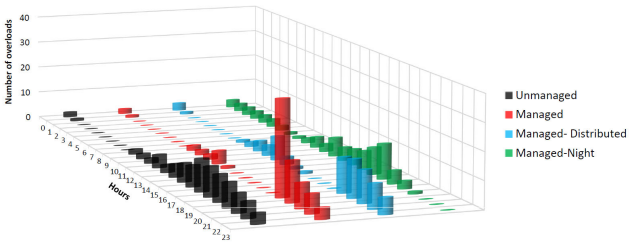

FIGURE 38. The 90th percentile of overloads by hours under unmanaged and managed charging scenarios.

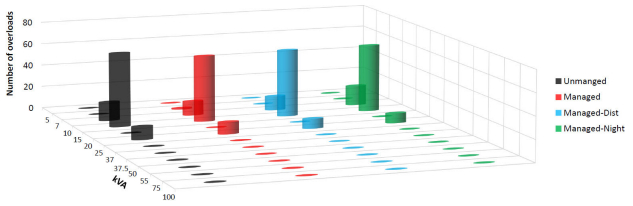

FIGURE 39. The 90th percentile of overloads be transformer power ratings under unmanaged and managed charging scenarios.

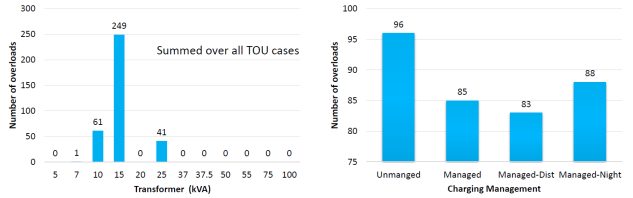

FIGURE 40. The 90th percentile of overloads versus transformer power ratings and charging management strategies, at various transformer power ratings (the left figure), and With various charging management strategies (the right figure).

hours (6 AM-6 PM). Accordingly, the hourly overloads under the four various scenarios (see Table 19) is shown in Fig. 38. It shows that the number of overloads is significantly reduced with the two alternative TOU assumptions. Likewise, the number of overloads at various transformer power ratings under unmanaged and managed charging scenarios is shown in Fig. 39. Again, the 15 kVA power transformers suffer from the most overloading. The summed number of total overloads over all TOU scenarios is shown in Fig. 40 (left), and the number of overloads at various charging management strategies is shown in Fig. 40 (right).

B. AGING ANALYSIS OF DISTRIBUTION TRANSFORMER DUE TO OVERLOAD

In addition to the aforementioned analysis based on the HotSpotter probabilistic assessment method, lifetime

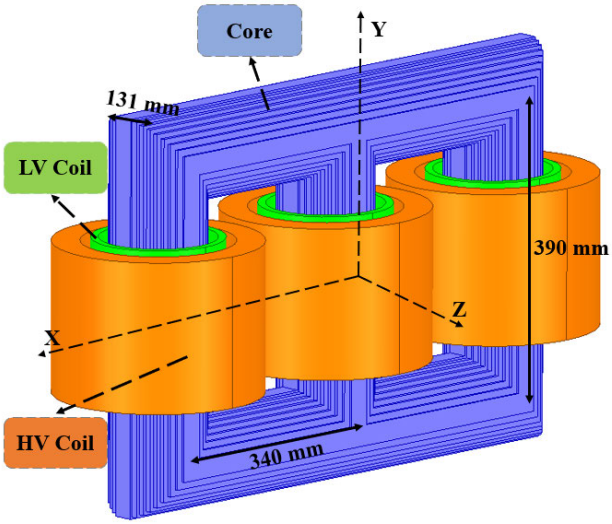

FIGURE 41. Topology and dimensions of the distribution transformer under investigation.

TABLE 20. Main parameters of the distribution transformer.

Parameter	Value
Apparent Power	100 kVA
HV Rating	33 kV
LV Rating	0.4 kV
Frequency	60 Hz
Type of Cooling	ONAN

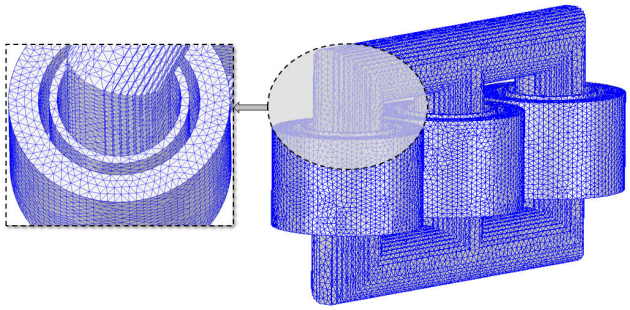

FIGURE 42. Finite element meshes of the distribution transformer model.

TABLE 21. Loss components in different loading scenarios.

Load Percentage	100 %	110 %	125 %	150 %
Load Loss (W)	1905	2156	2447	3106
Volumetric Core Loss Density (W/m^3)	5603	5603	5603	5603
HV Winding Loss Density (W/m^3)	26,416	29,916	33,916	43,083
LV Winding Loss Density (W/m^3)	75,476	85,476	96,904	123,095

derating of a distribution transformer is also investigated as an examplary distribution asset at various overloading conditions due to EV charging. Specifically, when a transformer is overloaded, its power losses increase and the hot-spot temperature (HST) in the transformer rises with respect to the nominal condition. Such increased HST is the main cause of winding insulation degradation which results in a reduction of the lifetime of the transformers, and eventually may lead to systematic failures. A 100 kVA distribution transformer is considered as the case study in this section. Multi-physics analysis is carried out to show the impact of overload on transformer temperature distribution and lifetime degradation. Specifically, Ansys Maxwell software is utilized to extract the electromagnetic losses of the transformer i.e., winding ohmic and core losses based on time-stepping finite element analysis (FEA). After that, Ansys Thermal module is leveraged to calculate the temperature distribution and HST of the transformer. Finally, lifetime estimation for different loading conditions of the transformer is carried out to characterize the transformer lifetime reduction.

1) ELECTROMAGNETIC ANALYSIS

The geometry of the distribution transformer under investigation along with the dimensions is shown in Fig. 41. the laminated magnetic core is used to reduce the eddy current losses and low-voltage (LV) coils are placed inside the high-voltage (HV) coils to minimize the leakage flux and copper cost. Table 20 shows the main parameters for the distribution transformer [29]. Time-stepping FEA technique is utilized to determine the performance characteristics of the transformer. Fig. 42 shows the FEA mesh of the 3D model which consists of 532,678 elements.

Table 21 summarizes the loss components in transformer parts under different loading conditions. The implementation of overload operation is chosen based on the IEEE Standard C57.91 [30]. These losses are used as the input for the subsequent thermal analysis and act as the heat sources in the thermal modeling.

2) THERMAL ANALYSIS

The cooling type of the transformer is oil natural air natural (ONAN), which circulates the oil and air naturally within the transformer tank based on natural convection phenomenon. Volumetric loss densities provided in Table 21 are the heat sources for the thermal simulation. These loss components heat up the active parts in the transformer, specifically, the magnetic core, high-voltage and low-voltage winding. Fig. 43 shows the temperature distribution under the condition of 40 ° C ambient temperature in the whole geometry of the transformer. As shown in Fig. 43, the middle leg of the core has higher temperature compared to other sections in the core, and the temperature along the height of the model increases in the coils. When low-temperature oil passes through the conductors, it is heated up and its cooling capability is reduced. As a result, HST occurs near the top where the oil exits. At last, the high-temperature oil dissipates its heat to the tank and radiators and eventually is cooled down again. The cooled oil then moves down in the tank due to higher density and the cooling cycle continues. Another observation

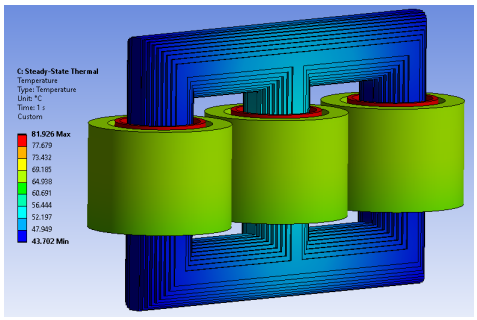

(a)

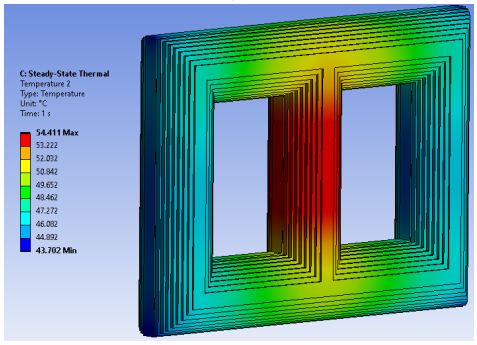

(b)

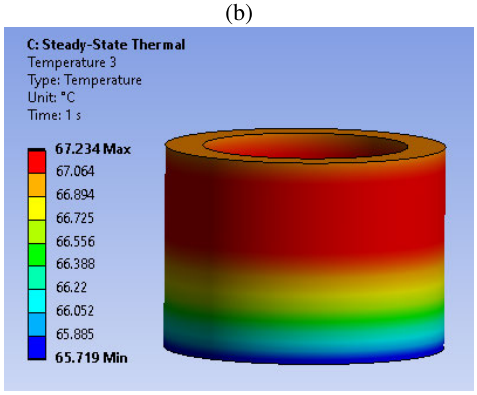

(c)

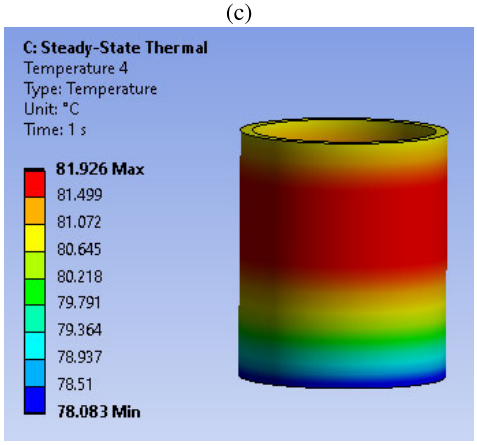

(d)

FIGURE 43. Temperature distribution of the transformer a) whole geometry, and b) magnetic core, c) HV windings and d) LV windings at 100% loading.

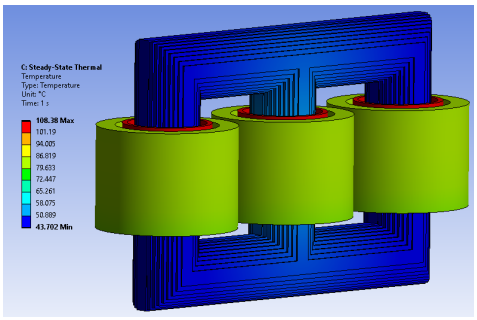

(a)

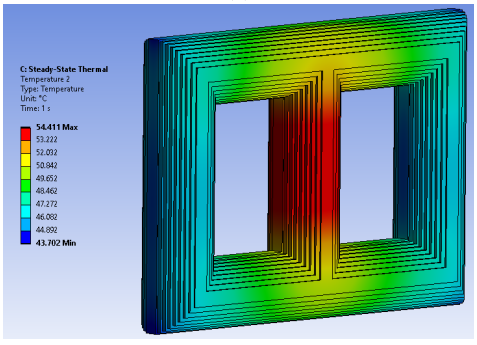

(b)

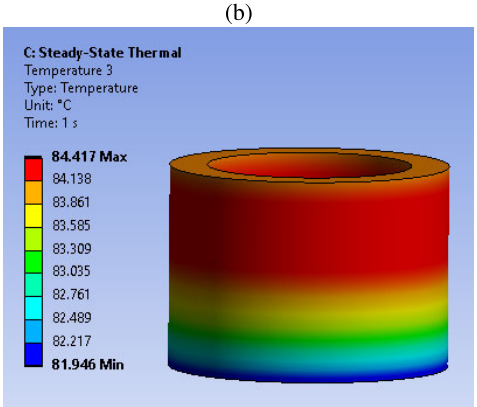

(c)

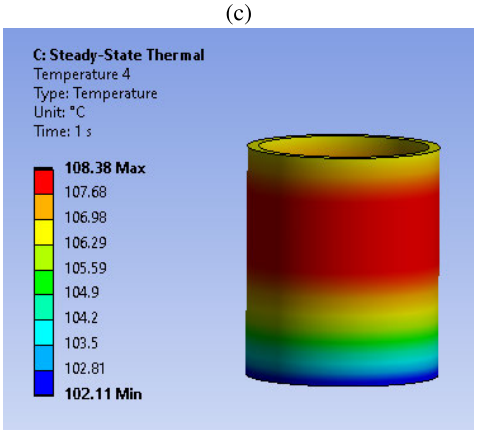

(d)

FIGURE 44. Temperature distribution of the transformer a) overall geometry, and b) magnetic core, c) HV winding and d) LV winding at 150% loading.

TABLE 22. Transformer HST under different loading conditions.

Load Percentage	100 %	110 %	125 %	150 %
HST in Whole Geometry (°C)	81.9	87.4	93.8	108.3
HST in Core (°C)	54.4	54.4	54.4	54.4
HST in HV Coil (°C)	67.2	70.8	74.9	84.4
HST in LV Coil (°C)	81.9	87.4	93.8	108.3

TABLE 23. Corresponding lifetime reduction in different loading conditions.

Load Percentage	100 %	110 %	125 %	150 %
HST (°C)	81.9	87.4	93.8	108.3
Per Unit Life	1	0.5246	0.2538	0.0536
Aging Acceleration Factor	1	1.906	3.94	18.65

is the higher temperature of LV winding in comparison with the HV windings since the loss density in LV windings is higher than that of the HV windings. Fig. 44 also shows the temperature distribution in different parts of the transformer under 150% loading condition in which the HST is increased significantly in both LV and HV windings due to higher loss density. Table 22 summarizes the HST in different parts of the transformer for the considered loading conditions.

3) TRANSFORMER LIFETIME ESTIMATION

The existing IEEE standards such as C57.91 [30] recommends that the relation of insulation deterioration to time and temperature follows an adaptation of the Arrhenius model, as follows [30]:

$$PUL = A \times e^{\frac{B}{T_{hst}+273}} \tag{1}$$

where PUL is the Per Unit Life, T_{hst} is the winding hottest spot temperature and A and B are the constants.

Also, there is another definition for lifetime which is known by the aging acceleration factor, as follows [31]:

$$F_{AA} = e^{\frac{15000}{383} - \frac{15000}{T_{hst}+273}} \tag{2}$$

The corresponding lifetime estimation for loading conditions is provided in Table 23. It is evident that the rate of lost life is increased exponentially by the increase in the HST. For instance, the aging acceleration factor in 150% loading is 18.65 which means that the transformer will age 18 times faster with respect to the nominal load. It is worth mentioning that these numbers are obtained assuming that the transformer is under persistent overload condition. Although this is not the case in real-world applications, the values in Table 23 are instructive benchmarks to understand the effects of overload on lifetime degradation of the transformers.

C. TRANSFORMER SIZING RECOMMENDATION

From Section IV-A, the WKRECC transformers statistics is presented in Table 24. It is evinced from the HotSpotter analysis results shown in Section IV-A that most of the overloading is likely to occur to transformers with ratings of 7 kVA, 10 kVA, 15 kVA and 25 kVA. Considering the potential prevalence of future EV charging rate of 10-20 kW per EV, to avoid overloading for even charging a single EV, it may be advisable to simply upgrade all transformers of 5, 7 and 10 kVA to a larger rating. It may not be economically feasible to upgrade all 15 kVA and 25 kVA since they account for more than 80% of the assets. Thus, it may be desirable to use charging controllers to limit the EV charging rate for consumers served by these transformers.

TABLE 24. WKRECC transformers statistics.

Transformer rating (kVA)	5	7	10	15	20	25	50
Percentage of transformers (%)	0.1	0.1	2.6	47.8	0.1	33.1	14
Average residents per asset	1.0	1.0	1.1	1.2	2.0	1.8	3.0

In addition, to avoid transformer overloading for these serving multiple consumers, appropriate time-of-use schemes to incentivize consumers to charge their EVs at different times and spread their EV charging as much as possible would be helpful.

In the literature, many EV charging industry protocols and standards are reported to discuss safety, reliability, and interoperability issues. In this study, different EV charging standards and protocols are documented in Table 25 [32], [33], [34], [35], [36], [37], [38], [39], [40].

V. FUTURE RESEARCH

A. EV CHARGING STRATEGY RESEARCH

EV charging strategy plays an important role in determining the total effective EV power demand. Future research is needed to identify smart charging strategies and provide charging pricing programs, credits and incentives, etc.

B. CONSIDERATION OF EV DISCHARGING (V2G)

EVs could discharge energy into the power grid in addition to charging from the power grid. In a smart charging/discharging management system, a mechanism for coordination between EV charging and discharging is provided, which reduces EV integration impact on the system and enhances utilization of EV's ability to provide ancillary services to the grid. Future research could look into potential architectures, functional requirements, and optimization algorithms for implementing novel and practical smart charging/discharging management system.

C. HIGH-RESILIENCY [CHARGER + PV + ENERGY STORAGE] MICROGRID

Establishing a microgrid by integrating charging station, solar power generation, and energy storage (battery, hydrogen, etc.), might be a secure and sustainable approach for both utility grid and vehicle charging, especially under extreme weather conditions or during natural disasters. Such a microgrid system not only can provide ancillary services to the grid stability such as reactive power, voltage and frequency support, but also provides a secure and reliable charging

TABLE 25. Summary of different EV charging standards and protocols [32], [33], [34], [35], [36], [37], [38], [39], [40].

Organizations	Standards and Protocols
International Electrotechnical Commission (IEC)	IEC TC 21: battery management; IEC TC 69: EV charging infrastructure; IEC TC 64: electric installation.
IEEE	IEEE P1809: electric transportation guide; IEEE P2690: vehicle authorization; IEEE P2030: interoperability of smart grid; IEEE 519-2014: power quality standards; IEEE 2030.1.1: fast DC charging for EV.
National Fire Protection Association (NFPA)	NFPA 70B: maintenance for electrical equipment; NFPA 70: safety; NEC 625/626: EV charging systems.
Society of Automobile Engineers (SAE)	J1773: inductive coupled charging; J2894: power quality; J2836/2847/2931: communication; J1772: EV conductive charging.
Isolation and Technical Safety Standards (ITST)	DIN V VDE 0510-11: battery installation and secondary batteries; UL 2231: supply circuit protection; UL 2202: charging system protection; NFPA 70/70 E: branch circuit protection, workplace safety; IEC TC 69/64: electrical installation; ISO 6469-2:2009 (IEC): failure protection; SAE J-2464: recharge energy storage; SAE J-2344: EV safety.
Underwritters Laboratories (UL)	UL2594/2251,2201: electric vehicle supply equipment; UL 2231: safety.
International Organization for Standardization	ISO/CD 6469-3.3: safety; ISO 6469-1:2009: on-board rechargeable batteries.
Japan Electric Vehicle Association Standards (JEVS)	JEVS G101-109: fast charging; JEVS C601: EV charging plugs; JEVS D701: batteries.

infrastructure for EVs. Fundamental systematic simulation models, smart controls, and grid stability analysis, as well as the synergistic design optimization of a general 'charger+PV+energy storage' microgrid system might be necessary for utilities.

D. TRANSFORMER LIFETIME MODELING AND PREDICTION

With an increasing number of EVs deployed into the distribution network, the charging and discharging interaction with the distribution grid may inevitably pose overload stress on the distribution transformers over the long term, especially from the fast charging of megawatt-scale heavy-duty EVs such as Class-7 and Class-8 trucks. Frequent inrush currents from charging/discharging events may cause uneven temperature distribution in the transformer windings, resulting in winding hotspots, dielectric insulation degradation, or even intensive grid blackout. High-fidelity online predictive reliability models need to be developed and integrated for utility stakeholders to predict and monitor the health condition of the distribution transformers based on the deployed EVs and real-time mission profiles. The outcome of the transformer lifetime prediction can be integrated into the control systems (e.g., SCADA) of the charging stations.

VI. CONCLUSION

In this study, DRIVE software tool was used to evaluate the capacity of WKRECC circuits to meet future EV charging needs under assumed EV adoption scenarios. Possible overloading (i.e., thermal congestion) on the circuit and undervoltage violation are examined. Here, the impact of the intensive charging of EVs on distribution transformers has been investigated. The investigation based on the HotSpotter software concludes that: (1) The TOU structure significantly affects the transformer overloading in the system. (2) With managed EV charging strategies, the number of transformer overloading decreases significantly. (3) Distributed managed charging spreads the charging and prevents the high number of overloads immediately after TOU hours. (4) Increased overloads observed at night by shifting 80% of demand from the evening (6 PM to 12 AM) to night charging.

Also, in this paper, the impact of EV charging overload on a 100 kVA distribution transformer was investigated. Multi-physics analysis was performed in Ansys Maxwell and Thermal module to acquire the electromagnetic losses and temperature distribution of the transformer, respectively. It was found that losses have increased with the increase in the loading of the transformer. Consequently, HST has also increased due to overload conditions. The lifetime estimation for different loading conditions of the transformer was conducted. Since the lifetime estimation is based on HST, an increase in HST due to overloading caused considerable lifetime degradation, which eventually leads to accelerated aging of the transformer.

REFERENCES

[1] *Office of Energy Efficiency & Renewable Energy*, Department of Energy, Washington, DC, USA, 2023. [Online]. Available: https://afdc.energy.gov

[2] M. R. Khalid, I. A. Khan, S. Hameed, M. S. J. Asghar, and J.-S. Ro, "A comprehensive review on structural topologies, power levels, energy storage systems, and standards for electric vehicle charging stations and their impacts on grid," *IEEE Access*, vol. 9, pp. 128069–128094, 2021.

[3] K. Kaur, S. Garg, G. Kaddoum, S. H. Ahmed, F. Gagnon, and M. Atiquzzaman, "Demand-response management using a fleet of electric vehicles: An opportunistic-SDN-based edge-cloud framework for smart grids," *IEEE Netw.*, vol. 33, no. 5, pp. 46–53, Sep. 2019.

[4] H. Wu, M. Shahidehpour, A. Alabdulwahab, and A. Abusorrah, "A game theoretic approach to risk-based optimal bidding strategies for electric vehicle aggregators in electricity markets with variable wind energy resources," *IEEE Trans. Sustain. Energy*, vol. 7, no. 1, pp. 374–385, Jan. 2016.

[5] S. Shafiee, M. Fotuhi-Firuzabad, and M. Rastegar, "Investigating the impacts of plug-in hybrid electric vehicles on power distribution systems," *IEEE Trans. Smart Grid*, vol. 4, no. 3, pp. 1351–1360, Sep. 2013.

[6] S. Faddel, T. Youssef, A. T. Elsayed, and O. A. Mohammed, "An automated charger for large-scale adoption of electric vehicles," *IEEE Trans. Transport. Electrific.*, vol. 4, no. 4, pp. 971–984, Dec. 2018.

[7] S. Deilami, A. S. Masoum, P. S. Moses, and M. A. S. Masoum, "Real-time coordination of plug-in electric vehicle charging in smart grids to minimize power losses and improve voltage profile," *IEEE Trans. Smart Grid*, vol. 2, no. 3, pp. 456–467, Sep. 2011.

[8] O. Sundstrom and C. Binding, "Flexible charging optimization for electric vehicles considering distribution grid constraints," *IEEE Trans. Smart Grid*, vol. 3, no. 1, pp. 26–37, Mar. 2012.
[9] A. O'Connell, D. Flynn, and A. Keane, "Rolling multi-period optimization to control electric vehicle charging in distribution networks," *IEEE Trans. Power Syst.*, vol. 29, no. 1, pp. 340–348, Jan. 2014.
[10] S. Weckx, R. D'Hulst, B. Claessens, and J. Driesensam, "Multiagent charging of electric vehicles respecting distribution transformer loading and voltage limits," *IEEE Trans. Smart Grid*, vol. 5, no. 6, pp. 2857–2867, Nov. 2014.
[11] J. de Hoog, T. Alpcan, M. Brazil, D. A. Thomas, and I. Mareels, "Optimal charging of electric vehicles taking distribution network constraints into account," *IEEE Trans. Power Syst.*, vol. 30, no. 1, pp. 365–375, Jan. 2015.
[12] J. de Hoog, T. Alpcan, M. Brazil, D. A. Thomas, and I. Mareels, "A market mechanism for electric vehicle charging under network constraints," *IEEE Trans. Smart Grid*, vol. 7, no. 2, pp. 827–836, Mar. 2016.
[13] X. Zhu, B. Mather, and P. Mishra, "Grid impact analysis of heavy-duty electric vehicle charging stations," in *Proc. IEEE Power Energy Soc. Innov. Smart Grid Technol. Conf. (ISGT)*, Feb. 2020, pp. 1–5.
[14] A. Jenn and J. Highleyman, "Distribution grid impacts of electric vehicles: A California case study," *iScience*, vol. 25, no. 1, Jan. 2022, Art. no. 103686.
[15] M. Kamruzzaman and M. Benidris, "Effective accessible energy to accommodate load demand of electric vehicles," in *Proc. IEEE Ind. Appl. Soc. Annu. Meeting (IAS)*, Sep. 2018, pp. 1–8.
[16] M. Alturki and A. Khodaei, "Marginal hosting capacity calculation for electric vehicle integration in active distribution networks," in *Proc. IEEE/PES Transmiss. Distrib. Conf. Expo. (T&D)*, Apr. 2018, pp. 1–9.
[17] J. Zhao, J. Wang, Z. Xu, C. Wang, C. Wan, and C. Chen, "Distribution network electric vehicle hosting capacity maximization: A chargeable region optimization model," *IEEE Trans. Power Syst.*, vol. 32, no. 5, pp. 4119–4130, Sep. 2017.
[18] M. Lillebo, S. Zaferanlouei, A. Zecchino, and H. Farahmand, "Impact of large-scale EV integration and fast chargers in a Norwegian LV grid," *J. Eng.*, vol. 2019, no. 18, pp. 5104–5108, Jul. 2019.
[19] S. Wang, C. Li, Z. Pan, and J. Wang, "Probabilistic method for distribution network electric vehicle hosting capacity assessment based on combined cumulants and Gram–Charlier expansion," *Energy Proc.*, vol. 158, pp. 5067–5072, Feb. 2019.
[20] A. Nagarajan and Y. Zakai, "Data validation for hosting capacity analyses," Nat. Renew. Energy Lab. (NREL), Golden, CO, USA, Tech. Rep. NREL/TP-6A40-81811, 2022.
[21] S. S. Letha and M. Bollen, "Impact of electric vehicle charging on the power grid," Luleå Univ. Technol., Luleå, Sweden, Tech. Rep. ISSN 1402-1536, 2021.
[22] C. Warren, "EPRI tool helps utilities assess 'hosting capacity' on distribution systems," *EPRI J.*, Oct. 2019. Accessed: Jan. 5, 2023. [Online]. Available: https://eprijournal.com/the-host-with-the-most/
[23] *West Kentucky Rural Electric*. Accessed: Jul. 10, 2022. [Online]. Available: https://www.wkrecc.com
[24] *Grid Integration Tech Team and Integrated Systems Analysis Tech Team*, Summary Report on EVs at Scale and the U.S. Electric Power System, U.S. Dept. Energy, Washington, DC, USA, 2019.
[25] L. Slezak, "FY2010 annual progress report for vehicle and systems simulation and testing," Office Energy Efficiency Renew. Energy (EERE), Washington, DC, USA, Tech. Rep. DOE/EE-0703, 2011.
[26] *DRIVE Applications for Planning and Screening*, EPRI, Washington, DC, USA, 2023.
[27] *DRIVE Brochure*, EPRI, Washington, DC, USA, Feb. 2022.
[28] C. Warren. *Spotting the HotSpots*. Accessed: Oct. 3, 2022. [Online]. Available: www.eprijournal.com/spotting-the-hotspots/
[29] B. C. Sujatha, T. V. Ramaswamy, R. R. Prabhu, N. Sumana, and S. Z. Ismail, "Design of 100kVA energy efficient three phase hybrid transformer for combined application of solar and wind," in *Proc. 4th Int. Conf. Converg. Technol. (I2CT)*, Oct. 2018, pp. 1–4.
[30] *IEEE Guide for Loading Mineral-Oil-Immersed Transformers and Step-Voltage Regulators*, Standard C57.91-2011 (Revision of IEEE Std C57.91-1995), Mar. 2012, pp. 1–123.
[31] *IEEE Standard Test Procedure for Thermal Evaluation of Insulation Systems for Liquid-Immersed Distribution and Power Transformers*, Standard C57.100-2011 (Revision IEEE Std C57.100-1999), 2012, pp. 1–37.
[32] M. C. Falvo, D. Sbordone, I. S. Bayram, and M. Devetsikiotis, "EV charging stations and modes: International standards," in *Proc. Int. Symp. Power Electron., Electr. Drives, Autom. Motion*, Jun. 2014, pp. 1134–1139.
[33] A. Oron, *Top 10 Countries in the Global EV Revolution: 2018 Edition*. Inside EVs, Miami, FL, USA, 2020.
[34] *Society of Automation Engineering-International Standards on EV Charging Stations*. Accessed: Jan. 20, 2023. [Online]. Available: https://www.sae.org/
[35] *IEEE Standard for Interconnection and Interoperability of Distributed Energy Resources With Associated Electric Power Systems Interfaces*, Standard 1547-2018, 2018.
[36] UL. *Electric Vehicle Infrastructure Services-UL*. Accessed: Jan. 20, 2023. [Online]. Available: https://www.ul.com/
[37] *National Electrical Code*, National Fire Protection Association, Quincy, MA, USA, 1915, vol. 70.
[38] *Electric Vehicle Charging Stations-Standards*. Accessed: Jan. 22, 2023. [Online]. Available: https://www.iso.org/
[39] *CHAdeMO Protocol Development*. Accessed: Jan. 22, 2023. [Online]. Available: https://www.chademo.com
[40] *IEC-Electric Vehicles Charging Stations*. Accessed: Jan. 25, 2023. [Online]. Available: https://www.iec.ch

PRANOY ROY (Member, IEEE) received the B.Sc. degree in electrical and electronics engineering from the Rajshahi University of Engineering and Technology, Bangladesh, the M.Sc. degree in engineering technology from Western Carolina University, Cullowhee, NC, USA, and the Ph.D. degree in electrical engineering from the University of Kentucky, Lexington, KY, USA, focusing on high-performance renewable energy and power electronic systems. He is currently a Lead Engineer with Eaton Research Labs, USA. He has published around 20 peer-reviewed journal and conference papers.

REZA ILKA (Graduate Student Member, IEEE) received the M.Sc. degree in power engineering from the Babol University of Technology, in 2012, and the Ph.D. degree in power engineering from Semnan University, in 2018. He is currently pursuing the second Ph.D. degree with the University of Kentucky, focusing on the analysis, design, and optimization of electrical machines and magnetic components. He was an Electromagnetic Design Engineer with the Research and Development Division, MAPNA Group, Iran, for five years. He has published several journal and conference papers in electrical machines and drives.

JIANGBIAO HE (Senior Member, IEEE) received the Ph.D. degree in electrical engineering from Marquette University, Milwaukee, WI, USA. He is currently with the Department of Electrical and Computer Engineering, University of Kentucky, USA. Previously, he was with the industry, most recently as a Lead Engineer with GE Global Research, Niskayuna, NY, USA. He was also with Eaton Corporation and Rockwell Automation, before he joined GE Global Research, in 2015. He has authored and coauthored over 120 technical papers and ten U.S. patents. His research interests include transportation electrification, renewable energies, and fault-tolerant electric power apparatuses for safety-critical applications. He was a recipient of the 2019 AWS Outstanding Young Member Achievement Award recognized by the IEEE Industry Applications Society. He has served as an editor or an associate editor for several prestigious IEEE journals in the electric power area. He also served in various roles in the organizing committees for numerous IEEE conferences. He has been an active member of multiple IEEE standards working groups.

YUAN LIAO (Senior Member, IEEE) received the bachelor's and master's degrees from Xi'an Jiaotong University, the second master's degree from the National University of Singapore, and the Ph.D. degree from Texas A&M University, College Station, TX, USA. He was a Consulting Research and Development Engineer and then a Principal Consulting Research and Development Engineer with the Corporate Research Center, ABB Inc., Raleigh, NC, USA, from 2000 to 2005. He is currently a Professor holding the endowed Blazie Family professorship with the Department of Electrical and Computer Engineering, University of Kentucky, Lexington, KY, USA, and the Director of the Graduate Certificate Programs with the Power and Energy Institute of Kentucky. His research interests include power system protection, analysis and planning, smart grid, and renewable energy integration.

AARON M. CRAMER (Senior Member, IEEE) received the B.S. degree (summa cum laude) in electrical engineering from the University of Kentucky, Lexington, KY, USA, in 2003, and the Ph.D. degree from Purdue University, West Lafayette, IN, USA, in 2007. From 2007 to 2010, he was a Senior Engineer with PC Krause and Associates, West Lafayette, IN, USA. In 2010, he joined the University of Kentucky, where he is currently a Professor. His research interests include simulation, control, and optimization of power and energy systems.

JUSTIN MCCANN (Member, IEEE) received the bachelor's degree in business education from Southern Illinois University, Carbondale, in 2003, and the bachelor's degree in electrical engineering from The University of Memphis, in 2006. He is currently the Vice President of Engineering with West Kentucky Rural Electric Cooperative Corporation, Mayfield, KY, USA. Previously, he was the Vice President of Engineering with Today's Power, subsidiary of the Electric Cooperative of Arkansas, where his work included projects to develop utility scale solar and battery energy storage, as well as planning and testing electric vehicle charging infrastructure. He was also a Principal and Managing Member with Fisher Arnold and Midsouth Utility Consultants. He has 20 years of engineering and leadership experience, including more than 15 years in the electric utility industry developing comprehensive system and financial planning and design projects. He is a registered professional engineer in several states. He is a member of the National Rural Electric Cooperative Association Transmission and Distribution Engineering Committee, Milsoft National Engineering Analysis Advisory Board, Tennessee Valley Public Power Association Research and Development Committee, and several other regional boards and committees.

SAMUEL DELAY received the B.S. degree in electrical engineering from The University of Tennessee, Knoxville, TN, USA, and the M.B.A. degree from The University of Tennessee at Chattanooga, Chattanooga, TN, USA. He is currently a Senior Program Manager with TVA Strategic Research-Technology Innovation. His research interests include customer technology, new business and grid services operations research and support, and technology innovation.

STEVEN COLEY received the bachelor's and the M.S./M.B.A. degrees in mechanical engineering from The University of Tennessee, Knoxville, in 2010 and 2012, respectively. He is currently the Manager of Grid Research and Development with Tennessee Valley Authority, USA. He leads a team focused on research and development activities for the TVA transmission systems, local power company distribution systems, and end-use technologies.

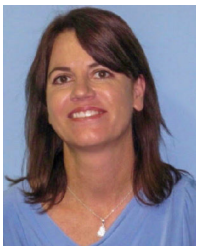

MELISSA GERAGHTY received the B.S. degree in ecology and evolutionary biology from The University of Tennessee, Knoxville, TN, USA, and the M.A.S. degree in geographic information systems from Arizona State University, Tempe, AZ, USA. She is currently an Engineer Scientist III with the Electric Transportation Program (P18), Electric Power Research Institute (EPRI). Her research interests include electric vehicles and all things included, such as charging infrastructure, battery technologies, and electric grid.

SACHINDRA DAHAL received the B.S. degree in civil engineering from Tribhuvan University, Nepal, and the master's and Ph.D. degrees in civil and environmental engineering from the University of Illinois Urbana–Champaign. His Ph.D. research focused on lane keeping of autonomous vehicles in adverse weather conditions. He is currently an Engineer Scientist with the Electric Power Research Institute (EPRI). His current projects involve grid impact analysis due to EV load, EV future trend projection, and V2B demonstration projects.